Physics – Uspekhi **41** (4) 379 – 402 (1998)

REVIEWS OF TOPICAL PROBLEMS PACS numbers: **31.50.+w**, 31.70 Hq, 33.70.Fd, 42.55.Gp, 82.40.Tc

Vibrational relaxation of excimers

V V Datsyuk, I A Izmaĭlov, V A Kochelap

Contents

Abstract. A review of the vibrational relaxation of excimers is presented. Various kinetic models used in the literature to interpret experimental data and to model excimer lasers are discussed. Of these, those based on the Fokker – Planck diffusion equation are the most general due to the essentially nonequilibrium population of the hundreds of high vibrational levels and because of the multiquantum nature of the transitions involved. Numerous manifestations of these important kinetic features are analyzed. The diffusive relaxation concept has led to an overestimate of the influence of vibrational relaxation on excimer laser parameters, the saturant light flux and quantum yield expressions departing considerably from those commonly used. To gain insight into relaxation physics, considerable attention is given to the determination of kinetic parameters capable of adequately describing the electronic-vibration kinetics. Rate constants for excimer vibrational relaxation are also given.

V V Datsyuk Department of Physics, T Shevchenko Kiev University, ul. Vladimirskaya 64, 252017 Kiev, Ukraine
Tel. (380-44) 266 44 77
Fax (380-44) 266 40 36
E-mail: teamoptp@pd.ups.kiev.ua
I A Izmaĭlov, V A Kochelap Institute of Semiconductor Physics, National Academy of Sciences of the Ukraine, prosp. Nauki 45, 252650 Kiev, Ukraine
Tel. (380-44) 265 77 78
E-mail: class@semicond.kiev.ua

Received 28 May 1996, revised 5 December 1997
Uspekhi Fizicheskikh Nauk **168** (4) 439 – 464 (1998)
Translated by Yu V Morozov; edited by A Radzig

1. Introduction

Developments in laser physics during the last decades have been crowned with the advent and further improvement of excimer lasing systems, the most powerful and effective of all UV lasers [1 – 12]. At present, great efforts are being made to improve the KrF excimer light amplifier to be used in a laser thermonuclear fusion facility [13 – 17]. The Rutherford Appleton Laboratory [15] has already achieved a radiance of order 10^{20} W cm^{-2} sr^{-1} and demonstrated the possibility of raising it to 10^{22} W cm^{-2} sr^{-1}. For a light intensity of 10^{21} W cm^{-2}, the electric field strength is approximately 10^{14} V m^{-1}. This is 100 times greater than the strength of the Coulomb field binding an electron in a ground-state hydrogen atom. Harnessing such high-power radiation has had revolutionary effect on the progress in atomic and plasma physics since the late 80s [18].

The advent and development of excimer lasers has been supported by extensive investigations of excimers, i.e. diatomic molecules (dimers) stable only in the excited state [4]. A wealth of data has been obtained from experimental studies of luminescence spectra and the kinetics of electronically excited states of rare-gas halides (RgX). However, some theoretical aspects of excimer kinetics have not yet been adequately described. Specifically, there is a gap in the understanding of the kinetics of vibrational relaxation of excimers.

Investigations of vibrational relaxation in excimer laser modelling were frequently substituted by simplified approximations, one of the most widely employed being the concept of an equilibrium molecular distribution over vibrational levels. However, this approach ignores a number of experimental and theoretical findings. It was shown back in 1979 that a part of the KrF(B) excimers in a KrF laser populate high vibrational levels and do not contribute to light amplification [19–21]. Many phenomenological models of active media, taking into consideration vibrational relaxation, make use of VT-relaxation rate constants which are in fact adjustable parameters of these models [9, 10, 22]. It is generally accepted that there are universal kinetic parameters for excimers such as quenching rate constants K_Q and effective radiative lifetimes τ_{re}. In other words, it is believed that the time τ_{re} for a molecule measured in one experiment must be just the same in another experiment. However, the Einstein coefficients for spontaneous RgX(B, C) phototransitions are known to depend on the vibrational energy [23–25]; therefore, τ_{re} must be a function of the vibrational distribution of molecules.

Also, it should be emphasized that theoretical interpretations of experimental findings are sometimes conflicting. Here is an example illustrating the discrepancy. Studies [14, 26, 27] on active media of XeCl excimer amplifiers revealed a nanosecond recovery for the gain coefficient following propagation of a short saturant light pulse through the active medium. The experimental results [26] were explained in two mutually exclusive ways [26, 28]. It was first supposed that the measured time τ_s of the gain recovery approximately equals the $XeCl^*$ quenching time [26]. Later, however, it was concluded that τ_s is equivalent to the vibrational relaxation time of $XeCl^*$ [28].

It is clear from the above discussion that the distribution of excimers over vibrational levels needs to be thoroughly investigated. It is worthwhile to note that the Soviet school of physics has made a fundamental contribution to the development of the vibrational relaxation theory [29–46]. Some of these results are used in the present review. Specific features of excimer relaxation include a markedly nonequilibrium molecular distribution over vibrational energy levels and multiquantum character of transitions. Some approaches to the construction of vibrational relaxation models are considered in Section 2. The validity of a method for studying relaxation kinetics certainly depends on the knowledge of the vibrational relaxation rate constants k_{VT}. The corresponding values for excimer molecules are summarized in Tables 2–4 (Section 4). When using these constants, it should be borne in mind that the term vibrational relaxation rate constant is employed to define parameters having essentially different physical meanings. Section 3 discusses characteristic features of typical quasi-steady-state distributions of excimers throughout vibrational energy levels. Section 5 deals with the influence of vibrational relaxation kinetics on the performance of excimer lasers. Effects of plasma electrons in excimer lasers on the kinetics of relaxation processes are considered in Section 6. Moments of the vibrational energy distribution function calculated in Section 7 are harnessed to estimate deviations of vibrational populations from equilibrium for both time-averaged or steady-state processes (Section 7.1) and vibrational relaxation kinetics in the case of pulse excitation (Section 7.2). Section 8 illustrates the application of the diffusion approximation. The intensity of experimentally observed nonstationary $I_2(D' - A')$ luminescence is computed in Section 8.1. Section 8.2 analyzes experimental results on the dynamics of the gain recovery in an excimer amplifier of UV radiation. Section 9 is concerned with the effect of amplifying far IR radiation by RgX excimers arising from the nonequilibrium population of high vibrational levels. And, finally, Section 10 gives evidence that effective radiative lifetimes and the quenching rate constants of excimers should not in fact be regarded as constants. In the Conclusions, the importance of the physical phenomena reviewed in this paper is emphasized.

2. Vibrational relaxation models

Studies of excimer vibrational relaxation have employed several model representations. The simplest and most widely used models took advantage of the phenomenological approach. In these models, the set of all highly excited vibrational levels was considered as one energy state. More rigorous investigations required the electronic state to be divided into blocks of 4 to 20 vibrational levels each. Populations of such groups of levels were evaluated by means of numerical solution of level-to-level kinetic equations. Simple models allowing for correct analytical studies of different kinetic problems were constructed, based on the diffusion approximation.

It should also be emphasized that early studies [47, 20] have estimated the characteristic time-scale of vibrational relaxation without computing the population of selected vibrational levels. For example, the excitation of an I_2/Ar mixture by an electron beam of less than 40 ps duration resulted in the nonstationary luminescence of $I_2(D')$ molecules [47]. Examination of the spectral and kinetic characteristics of this luminescence allowed the vibrational relaxation time τ_v and radiative lifetime of $I_2(D')$ to be determined. The value of τ_v was derived from the comparison of quenching of luminescence with two light wavelengths, $\lambda_1 = 342$ and $\lambda_2 = 323$ nm. It is known that emission with λ_1 corresponds to the phototransition from the ground vibrational level of $I_2(D')$, while emission with λ_2 to that from the high vibrational level (the ninth one as according to Ref. [48]). Ref. [47] reports measurement of decay times $\tau(\lambda)$ for the two types of luminescence. The vibrational relaxation time was found from the following relation

$$\tau_v^{-1} = \tau^{-1}(\lambda_2) - \tau^{-1}(\lambda_1)\,. \qquad (1)$$

This formula was also used in Ref. [20]. Evidently, the involvement of many vibrational levels in the relaxation process accounts for the dependence of the relationship between $\tau(\lambda_2)$ and $\tau(\lambda_1)$ on several kinetic parameters. Therefore, the observed value of τ_v (1) may be considered as a very rough estimate of the vibrational relaxation rate.

2.1 Phenomenological models

In 1979, Jacob and co-workers [19, 21] measured intensity of $KrF(B \rightarrow X)$ fluorescence in the direction perpendicular to the axis of a KrF laser. The measurements were performed in the presence and absence of a laser radiation field. The results of the experiments indicated that a part of the KrF(B) molecules occupied high vibrational levels but failed to contribute to the stimulated laser emission. A simple phenomenological model was suggested to account for this observation.

The model considers the upper RgX^* laser level to be a combination of two sublevels, 1 and 2, which mix up as a result of collision with a buffer gas [10]. Sublevel 1 is normally the ground vibrational level of RgX(B) excimer, whilst sublevel 2 makes the set of all high vibrational levels of RgX(B, C) which do not contribute to light amplification. It is supposed that excimers are generated at sublevel 2. The two sublevels are subject to spontaneous and collisional decay. In addition, sublevel 1 decays due to field-induced transitions. The probability of transition from sublevel 1 to sublevel 2 per unit time is assumed to be $(1/\tau_v)(1-\theta_0)$, whereas the probability of reverse transition equals $(1/\tau_v)\theta_0$. Here, τ_v is the adjustable parameter called the vibrational relaxation time, and

$$\theta_0 \equiv \exp\left(-\frac{\varepsilon_0}{T}\right)\left[\sum_v \exp\left(-\frac{\varepsilon_v}{T}\right)\right]^{-1}$$

is the Boltzmann factor, ε_v is the energy of the vth vibrational level, and T is the gas temperature in energy units.

This phenomenological approach allows the population of a vibrational level involved in laser generation to be estimated from an equation of the form

$$\frac{dn_0}{dt} = -\frac{n_0 - \theta_0 N}{\tau_v} - \frac{n_0}{\tau_u} - \frac{\sigma\Phi}{h\nu}\, n_0 . \tag{2}$$

Here, N is the molecular concentration which can be derived from the following equation

$$\frac{dN}{dt} = -\frac{N}{\tau_u} + R - \frac{\sigma\Phi}{h\nu}\, n_0 . \tag{3}$$

Equations (2) and (3) include τ_u — the lifetime of an excimer, Φ (in W cm^{-2}) — the light flux in the active medium, σ — the stimulated emission cross-section, and $h\nu$ — the photon energy.

Equations (2) and (3) as well as their variants provided the basis for several studies [7–10, 22, 49–55]. Modified phenomenological models took into consideration the following processes: the contribution of a few low-lying KrF(B) vibrational levels to stimulated emission [22, 8, 53–55, 11], collisional mixing between RgX(B) and RgX(C) electronic states [51, 22, 9, 54, 55, 11], and interaction between RgX(B, C) excimers and plasma electrons [51, 55, 56].

2.2 Level-to-level kinetic models

In 1981, Dreiling and Setser [23] studied XeCl(B–X) and XeCl(C–A) emission spectra arising from the interaction of Xe($^3P_2$ or $^3P_1$) atoms and Cl_2, CCl_4, $COCl_2$ in the presence of He, Ne, Ar and N_2 at 0.1–15 mbar. In the majority of the experiments, the upper vibrational levels of excimers XeCl(B, C) were more fully populated than lower ones. The vibrational relaxation rate constants and energy conversion rates between B and C states were derived from the dependence of vibrational populations on the buffer gas pressure:

$$k_R = k_0 P_{ij}^R , \qquad k_T = k_0 P_{ij}^T . \tag{4}$$

Here, k_0 is the gas-kinetic collision rate constant, P_{ij}^R and P_{ij}^T are the probabilities of transitions in a single collision of a XeCl molecule with a buffer gas atom M:

$$\begin{aligned}
&RgX(B, j) + M \xrightarrow{P_{ij}^R} RgX(B, i) + M , \\
&RgX(C, j) + M \xrightarrow{P_{ij}^R} RgX(C, i) + M , \qquad (5)\\
&RgX(B, j) + M \xrightarrow{P_{ij}^T} RgX(C, i) + M , \\
&RgX(C, j) + M \xrightarrow{P_{ij}^T} RgX(B, i) + M . \qquad (6)
\end{aligned}$$

A similar approach was used in Ref. [25], which demonstrated the quasi-stationary chemiluminescence of KrF^* and $XeCl^*$ molecules. In this experiment, the effective relaxation rate constants were determined, taking into account both relaxation due to transitions between electronic states B and C, and VT transitions within the B state.

The use of an improved chemiluminescence technique is exemplified by a study on XeCl molecules [57]. The experiment was designed to populate certain vibrational levels, $XeCl(B, v = 0)$ and $XeCl(C, v = 0, 1)$. An exact population for a given vibrational level was achieved using photoassociation reactions between Xe and Cl atoms in the laser radiation field and also by laser excitation of the van der Waals XeCl(X) molecule. The recorded XeCl(B–X) and XeCl(C–A) fluorescence spectra proved to be time and wavelength resolved. The data obtained were applied to calculating rate constants for VT relaxation and mixing between electronic states B and C as well as radiative lifetimes and quenching rate constants of XeCl(B, C) states.

A theoretical examination of KrF^* relaxation in Ref. [24] was based on the numerical solution of level-to-level kinetic equations for the populations of all KrF(B) vibrational levels. The kinetic equations took into account recombination of Kr^+ and F^- ions which led to the population of the highest KrF(B) levels, vibrational VT transitions, spontaneous emission, collisional quenching, and stimulated emission from low-lying $KrF(B, 0 \leqslant v \leqslant 4)$ vibrational levels (Fig. 1). VT relaxation constants were obtained using a theoretical model of symmetric charge exchange between a Kr atom of the buffer gas and a Kr^+ ion of the KrF(B) molecule with ionic bonding. This model predicts a high rate of vibrational excitation loss in KrF(B): VT transitions are multiquantum (Fig. 2) and characterized by rate constants $k_{VT} \geqslant 10^{-10}$ cm^3 s^{-1}. In spite of this, vibrational relaxation proceeds so slowly, in compliance with the numerical solution of kinetic equations, that a part of the electron excitation is lost as a result of spontaneous emission and collisional quenching. Numerical calculation data [24] gave an insight into the effect of vibrational relaxation on the light generation process in a KrF laser [21].

To summarize the results of level-to-level kinetic studies, the following features of vibrational transitions need to be emphasized. In a single collision with a buffer gas atom, the RgX(B, C) molecule loses many vibrational quanta at once, and vibrational transitions may occur with a change of electronic state, i.e. from B to C or vice versa. By way of illustration, Table 1 shows the mean vibrational energy of $XeCl^*(v = 100)$ lost in a single collision. The $\langle \Delta\varepsilon_R \rangle$ values correspond to transitions without a change in the electronic

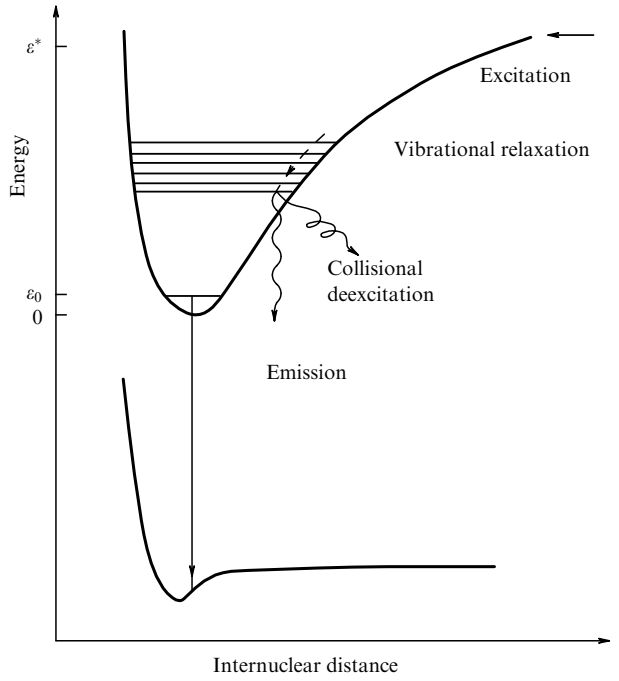

Figure 1. Schematic representation of excimer electronic terms and principal kinetic processes.

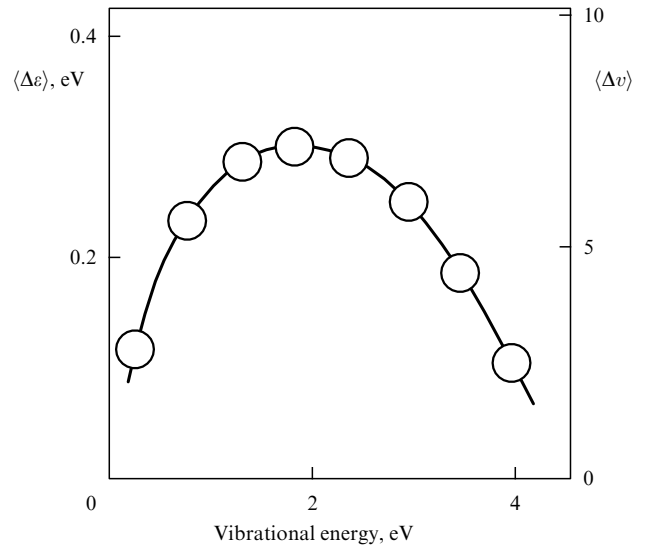

Figure 2. Mean energy transferred in the course of $Kr + KrF^*$ collisional events as a function of initial KrF^* vibrational energy [24].

Table 1. Some characteristics of reactions (5) and (6) involving $XeCl^*(v = 100)$, averaged over all collisions [23].

M	$\langle\Delta\varepsilon_R\rangle$, eV	$\langle\Delta v_R\rangle$	$\langle\Delta\varepsilon_T\rangle$, eV	$\langle\Delta v_T\rangle$
He	0.09	3.8	0.22	9.1
Ne	0.13	5.5	0.28	11.7
Ar	0.23	9.9	0.36	15.1
Kr	0.39	16.4	0.54	22.8

state (5), while $\langle\Delta\varepsilon_T\rangle$ values to transitions proceeded by state alteration (6). The table also presents estimates of average changes in the number of vibrational quanta of $XeCl^*$ in a single act of reaction (5) or (6). The value of $\langle\Delta v\rangle$ varies from 4 to 23 depending on the specific features of the process and the type of buffer gas. Analogous quantities are displayed in Fig. 2 illustrating the results of modelling collisions between KrF^* and Kr atoms [24]. It follows from Table 1 and Fig. 2 that vibrational relaxation of excimers is associated with multiquantum transitions and requires many collisions with buffer gas atoms. The excitation flow over vibrational levels of molecules can be described using the diffusion approximation.

2.3 Diffusion approximation

Vibrational transitions of molecules can be obviously regarded as the motion of excitation in a vibrational energy space. Modelling vibrational relaxation is possible using the Fokker – Planck diffusion equation [58, 35, 43, 44]. This equation has the form

$$\frac{\partial f}{\partial t} - \frac{\partial}{\partial\varepsilon} B(\varepsilon)\,\rho(\varepsilon)\left(\frac{\partial}{\partial\varepsilon}\frac{f}{\rho} + \frac{f}{T\rho}\right) + \tau_u^{-1}(\varepsilon) f = r(\varepsilon, t)\,. \qquad (7)$$

Here, $f(\varepsilon, t)$ is the distribution function introduced in such a way that it stands for the number of molecules within the vibrational energy range $(\varepsilon, \varepsilon + d\varepsilon)$ at the point in time t. $f(\varepsilon, t)$ normally describes the vibrational excitation in a cluster of collisionally mixed states. For instance, in the relaxation of inert gas halides RgX, B and C states are usually mixed up [20, 22, 25, 53, 59 – 62]. In this case, the vibrational distribution within one electronic state i is described by the function $f_i(\varepsilon, t) = \left(g_i / \sum_i g_i\right) f(\varepsilon, t)$, where g_i is the electronic degeneracy of i state. Specifically, for RgX(B, C) excimers $i = B, C$ and $g_B = g_C = 2$.

Equation (7) contains the diffusion coefficient $B(\varepsilon)$ and the vibrational state density $\rho(\varepsilon)$. In the region of low vibrational levels, the following approximate equality holds [36]:

$$B(\varepsilon) = \frac{T\varepsilon}{\tau_v}\,, \qquad (8)$$

which is used to determine the vibrational relaxation time τ_v or rate constant k_{VT}, $\tau_v^{-1} = k_{VT}[M]$, where [M] is the concentration of molecules (atoms) in the buffer gas M. The frequency $\tau_u^{-1}(\varepsilon)$ in Eqn (7) is a sum of probabilities of radiative and radiationless deexcitation of molecules (see Fig. 1). The generation of electronically excited molecules is characterized by the pumping rate $r(\varepsilon, t)$.

The Fokker – Planck equation is applicable when the molecular distribution over vibrational energy levels can be described by a smooth function ε:

$$\frac{1}{f}\frac{\partial}{\partial\varepsilon}\frac{f}{\rho} \ll 1\,.$$

According to Refs [44, 35], the Fokker – Planck equation for multiquantum processes shows a much higher generality compared with equations describing vibrational relaxation through one-quantum transitions. An advantage of diffusive relaxation models consists in the possibility of a simple analytical study of various kinetic problems. Specifically, the use of Eqn (7) allowed a number of known physical effects to be explained and new ones to be predicted [63 – 72]. In particular, the impact of vibrational relaxation on the excimer laser efficiency was analyzed. Also, these models were used to examine characteristics of excimer luminescence in the case of pulse excitation and the recovery of the gain coefficient in a pulse laser amplifier. It was demonstrated

that light amplification in active media of excimer lasers can be observed in both the UV and far IR regions [68]. Moreover, it was understood [72] why measuring one and the same kinetic parameter frequently yields different results depending on the measuring technique, the energy of generated electronically excited molecules, and the gas mixture composition.

3. Distribution of electronically excited molecules over vibrational energy levels

3.1 Characteristics of vibrational distributions

The most general problem of the vibrational relaxation theory centres around the computation of the function $f(\varepsilon_v, t)$, which describes the molecular distribution over vibrational energy levels. The distribution function can be found either numerically, by the solution of the system of level-to-level kinetic equations, or analytically, from the Fokker–Planck equation (7).

It seems appropriate to recall here some typical features of excimer relaxation essential for further discussion. The length of a pumping pulse (ca. 100 ns) in active media of excimer lasers is significantly longer than electronic-vibrational relaxation times; in particular, τ_u is of order 3 ns. Therefore, we may originally confine ourselves to the examination of quasi-stationary distributions of molecules over ε. By virtue of kinetic peculiarities, excimers are normally formed at high vibrational levels with the energy ε^* of order 5 eV. For this reason, we will be largely interested in the molecular distribution within a broad range of ε.

Both level-to-level kinetic models and the diffusion model predict similar patterns for the molecular distribution over vibrational energy levels. A typical vibrational distribution found with the help of the model for discrete vibrational levels [24] is presented in Fig. 3. The figure shows that the quasi-stationary distribution displays two silent features. On the one hand, the distribution in the region of high vibrational states is described by a smooth function of ε. On the other hand, the distribution of molecules over low vibrational levels is close to the high-temperature Boltzmann distribution.

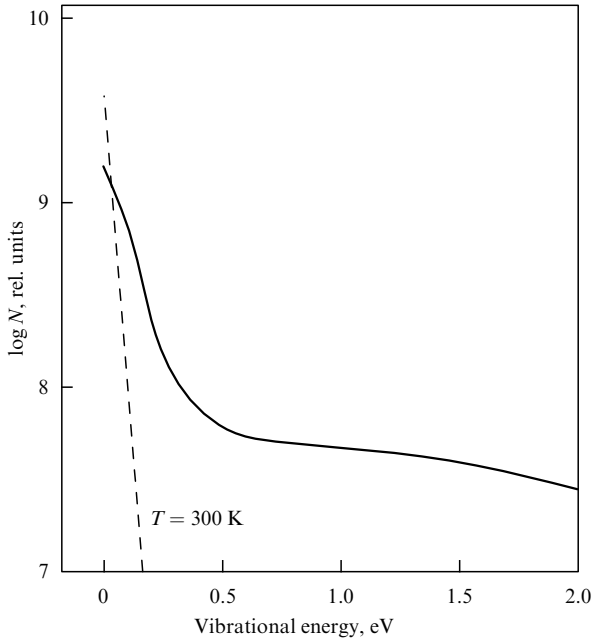

Figure 3. KrF(B) vibrational populations vs. vibrational energy [24]. The buffer gas (Kr) pressure constitutes 1 bar.

It ensues from the diffusion model that the vibrational distribution in the region of high vibrational states with $\varepsilon \gg T$ is described by a smooth function of ε [63]:

$$f(\varepsilon) = \frac{RT}{B(\varepsilon)} \exp\left[-\int_{\varepsilon}^{\varepsilon^*} \frac{T\,d\varepsilon}{\tau_u(\varepsilon)B(\varepsilon)}\right]. \quad (9)$$

Here, R is the rate of formation of molecules with energy ε^*, $r(\varepsilon) = R\delta(\varepsilon - \varepsilon^*)$. Specifically, approximations $B(\varepsilon) = T\varepsilon/\tau_v$ and $\tau_u = \text{const}$ being fulfilled, the distribution function (9) varies as $\varepsilon^{1-\tau_v/\tau_u}$. Therefore, the molecular distribution over a broad range of high vibrational states is substantially different from the equilibrium one.

3.2 Vibrational temperature

Let us consider relative populations of KrF(B) vibrational states in the limit of small vibrational energies $\varepsilon \ll D$, shown in Fig. 3 (D is the dissociation energy of a molecule). For the semilogarithmic scale of the figure, the Boltzmann distribution is represented by a straight line (the dotted line in Fig. 3 corresponds to the equilibrium distribution with $T_v = T = 300$ K). It follows from Fig. 3 that the distribution of molecules over low-lying vibrational levels is close to the Boltzmann distribution with $T_v > T$. Calculations made in Ref. [24] for buffer gas pressures $p = 0.5$, 1 and 2 bar, indicate that T_v decreases with increasing pressure, but the vibrational temperature markedly exceeds T at any p.

The diffusion model of vibrational relaxation predicts that the distribution function at low vibrational energies ($\varepsilon \ll D$) can be approximated by the function [72]

$$f(\varepsilon) = \frac{N}{T}\eta^v \exp\left(-\frac{\varepsilon}{T_v}\right), \quad (10)$$

where

$$T_v = \frac{T}{(1 - \tau_v/\tau_u)}, \quad (11)$$

$$\eta^v \equiv \exp\left[-\int_{T}^{\varepsilon^*} \frac{T\,d\varepsilon}{\tau_u(\varepsilon)B(\varepsilon)}\right]. \quad (12)$$

It will be shown below that the factor η^v takes into account the loss of molecules upon relaxation from high to low vibrational levels. In other words, the molecular distribution over low-lying vibrational states may be characterized by the Boltzmann function (10) with vibrational temperature $T_v > T$.

The inference of similarity between the molecular distribution over low-lying vibrational levels and the Boltzmann distribution agrees with the results of experimental studies on the luminescence spectra of XeCl(B–X) [59, 73] and KrF(B–X) [62, 74]. However, at a moderate buffer gas pressure ($p = 1-3$ bar), the observed emission spectrum of RgX(B–X) was reported to resemble the calculated spectrum for $T_v = T = 300$ K [73, 62, 74]. On the other hand, Ref. [26] reported an experimental study of the spectral distribution of the gain coefficient g in the active medium of a XeCl laser at a helium pressure of $p = 3$ bar. The authors evaluated the contribution of transitions $XeCl(B, v' = 1) \rightarrow XeCl(B, v'' = 1)$ and $XeCl(B, v' = 0) \rightarrow XeCl(B, v'' = 1)$ to g and determined $T_v \simeq 600$ K. Other studies of well-resolved XeF(B–X) luminescence spectra

over a broad pressure range of helium and neon [75, 76] also demonstrated the lack of thermalization of the XeF(B) distribution over vibrational levels right up to the buffer gas pressure of $p \simeq 4$ bar.

There is every reason to conclude that the approximation (10) obtained both analytically [72] and numerically [24] is in good qualitative agreement with experimental findings. At the same time, T_v values found experimentally when recording phototransitions from low vibrational levels of XeCl(B) and KrF(B) turned out to be different. This may be related to a weak dependence of the spectral profile for emission $B \to X$ on T_v, at least for the KrF excimer. In fact, for bound-free transitions of the type $KrF(B, v \to X)$, a rise in v from 0 to 4 does not result in an apparent variation of the spectral density of the Einstein coefficient [24], whereas the Boltzmann factor $\exp\left[-(\varepsilon_v - \varepsilon_0)/T\right]$ is reduced from 1 to 2×10^{-3}.

To summarize the analysis of $f(\varepsilon)$, it should be emphasized that formula (10) is applicable only to the low vibrational level region at $\tau_v < \tau_u$. As the vibrational energy rises, function (10) smoothly transforms to a power-like function (9). At low buffer gas pressures between 0 and 30 mbar, the inequality $\tau_v > \tau_u$ holds, i.e. vibrational relaxation proceeds more slowly than spontaneous emission. In this case, low vibrational levels are usually less populated than high ones [23], namely, population inversion occurs.

4. VT-relaxation rate constants

The reliability of a vibrational relaxation model is to a great extent dependent on the validity of the relaxation rate constants in use. Such constants for selected excimers are listed in Tables 2–4, which show their striking variations in similar kinetic processes. A more careful examination of the tables leads to the conclusion that the vibrational relaxation rate constants have different physical meanings. It is therefore important to know not only a k_{VT} value but also the formula which contains the given constant.

Table 2. VT-relaxation and VT-transition rate constants k_{VT}, 10^{-11} cm^3 s^{-1}.

Excimer	M	k_{VT}	Parameter	Ref.
ArF(B)	Ne	20	Parameter of Eqn (2)	[52]
$Cl_2(D')$	He	0.12	Reaction rate constant of $Cl_2^* + He \to Cl_2(v=0) + He$	[77]
HgBr(B)	He	2.0	Parameter of Eqn (7)	[78]
	Ne	2.0		
	Ar	7.7		
	N_2	15.3		
	Xe	28		
$I_2(D')$	Ar	2	Parameter of expression (1)	[47]
	Ar	2	Parameter of Eqn (7)	[64]
	SF_6	4		
	CF_4	10	Parameter of Eqn (7)	
	C_3F_8	22		
	C_5F_{12}	36		
XeBr(B)	Ar	2–100	$k^{BB}_{v,v'}$, $v = 30-150$	[79]
XeF(B)			$k^{BB}_{v,v-1} = vk_0$, $k^{BC}_{v,v'} = k_1 \exp\left[-(\varepsilon^B_v - \varepsilon^C_{v'})/T\right]$	[80]
	He	0.6	k_0	
	Ar	2		
	N_2	5		
	He	0.4	k_1	
	Ar	2		
	N_2	8		
XeF(B, C)	He	0.1	Thermalization rate constant for low vibrational levels	[76]
	Ne			

Table 3. VT-relaxation and VT-transition rate constants of KrF(B, C).

M	k_{VT}, 10^{-11} cm^3 s^{-1}	Parameter	Ref.
He	0.6 ± 0.3	Parameter of expression (1) with $\lambda_1 = 248.5$ nm and $\lambda_2 = 247, 246$ nm	[20]
Ar	5	Parameter of Eqn (2)	[21]
			[50]
			[10]
	4		[81]
			[53]
	4	Parameter of ten (2)-type equations for $\left[KrF(B, C, v = 0-4)\right]$	[22]
Kr	5	Parameter of Eqn (2)	[53]
	8		[10]
Kr		The sum of reaction rate constants over v' for $Kr + KrF^*(v) \to KrF^*(v') + Kr$	[24]
	10	$\varepsilon_v = 0-2$ eV	
	10–100	$\varepsilon_v = 2-4$ eV	
		$k'(j) \equiv k^{BB}_{ii-1} + k^{BC}_{ii-1}$, where i is the block of 9 vibrational levels	[25]
He	0.8 ± 0.5	$k'(v = 13)$	
	2.5 ± 0.5	$k'(v = 22)$	
	3.0 ± 0.7	$k'(v = 31)$	
	4.0 ± 1.2	$k'(v = 40)$	
Ne	1.2 ± 0.5	$k'(v = 13)$	
	2.5 ± 0.8	$k'(v = 22)$	
	3.5 ± 0.8	$k'(v = 31)$	
Ar	42 ± 12	$k'(v = 13)$	
	42 ± 23	$k'(v = 19)$	
	58 ± 12	$k'(v = 22)$	
	42 ± 17	$k'(v = 31)$	
Ar Kr	4 10	Parameter of Eqn (7)	[66]

4.1 Peculiarities of defining VT-relaxation rate constants

The scientific literature on modelling excimer lasers gives evidence of a few typical usages of the term vibrational (VT) relaxation rate constant. Firstly, this term is applied to the parameters of Eqn (2). Secondly, rate constants of transitions between vibrational levels of RgX(B, C) molecules (4) are sometimes called VT-relaxation rate constants. Thirdly, k_{VT} rate constants are introduced in the same way as in the diffusion model of vibrational relaxation [43]. Fourthly, certain studies designed to estimate k_{VT} (or τ_v) use measurements which show independence from the rates of transitions (5) and (6). For example, in Ref. [83] and later in Refs [22, 8, 53, 25] the term VT-relaxation time was employed for the time τ_s of the gain coefficient (g) recovery following propagation of a short light pulse through a KrF laser. However, the experiment [83] as well as modelling $g(t)$ with the aid of type (2) kinetic equations [22] and the vibrational relaxation diffusion model [84] demonstrated that τ_s is identical to the lifetime τ_u of KrF(B, C) excimers and does not depend on k_{VT}.

When using vibrational relaxation rate constants in phenomenological models, the following must be taken into account. On the one hand, the k_{VT} may be considered as adjustable parameters, neglecting molecular redistribution over high vibrational levels upon a change in the gas mixture

Table 4. VT-relaxation and VT-transition rate constants of XeCl(B, C).

M	k_{VT}, 10^{-11} cm^3 s^{-1}	Parameter	Ref.
Ar	10–15	Parameter of Eqn (2)	[49]
	5		[51]
		$k_R(j) \equiv \sum_{i<j} k_{ji}^{BB} = \sum_{i<j} k_{ji}^{CC}$, where j, i is the block of 4 vibrational levels	[23]
He	0.15–1.1–2.5–4.4	$k_R(4) - k_R(30) - k_R(70) - k_R(130)$	
Ne	0.5–2.9–6.2–9.5		
Ar	2.5–13–25–35		
Kr	0.6–2.7–5.5–7.3		
		$k_T(j) \equiv \sum_{i<j} k_{ji}^{BC} = \sum_{i<j} k_{ji}^{CB}$	
He	0.5–1.8–2.5–2.5	$k_T(4) - k_T(30) - k_T(70) - k_T(130)$	
Ne	0.7–2.6–3.5–3.5		
Ar	3.0–11–15–15		
Kr	3.0–11–16–16		
Xe		Reaction rate constant for	[57]
	20	$XeCl^*(v=2) + M \rightarrow XeCl^*(v=1,0) + M$	
	5.3	$XeCl(B, v=1) + M \rightarrow XeCl(C) + M$	
Ne	0.3–0.5	$k_{1,0}^{BB} - k_{0,1}^{BB}$	[28]
Ar		$k'(i) \equiv k_{ii-1}^{BB} + k_{ii-1}^{BC}$, where i is the block of m vibrational levels, $m = 20, 16, 11$	[25]
	17 ± 5	$k'(v = 33)$	
	31 ± 9	$k'(v = 60)$	
	43 ± 13	$k'(v = 75)$	
Ar		Reaction rate constant for	[82]
	10	$XeCl(B) + Ar \rightarrow XeCl(B, v=0) + Ar$	
	16	$XeCl(B) + Ar \leftarrow XeCl(B, v=0) + Ar$	
		Reaction rate constant for	[11]
Ne	7.7	$XeCl^{**} + Ne \rightarrow XeCl(B, v>1) + Ne$	
	2.3	$XeCl^* + Ne \rightarrow XeCl(C, v>2) + Ne$	
	3.0	$k_{v>1,\,v=0}^{BB}, k_{v>2,\,v=0,1}^{CC}, k_{v>1,\,v>2}^{BC}, k_{v=0,\,v=0,1}^{BC}$	
Xe	20	$k_{v>1,\,v=0}^{BB}, k_{v>2,\,v=0,1}^{CC}$	
	11	$k_{v>1,\,v>2}^{BC}, k_{v=0,\,v=0,1}^{BC}$	
He	0.8	Parameter of Eqn (7)	[71]
Ne	2		
Ar	5		
Kr	6		

composition, laser emission field, etc. The authors of Ref. [22, p. 4314] maintain that '... the kinetic equations should not be thought to describe exact physical processes of vibrational energy transfer ...'. Also, they further emphasize that the k_{VT} values found in their study are valid only for the sole concrete kinetic model.

On the other hand, it is easy to find the condition which, if fulfilled, ensures that the parameter τ_v^{-1} in Eqn (2) is related to the probabilities of elementary processes of energy transfer. This condition requires that the populations of vibrational levels with $v \neq 0$ be

$$n_v = \exp\left(-\frac{\varepsilon_v - \varepsilon_0}{T}\right)\frac{\theta_0(N - n_0)}{1 - \theta_0}\,. \tag{13}$$

Indeed, calculation of the rate of transitions between the ground ($v = 0$) and all other ($v \neq 0$) vibrational levels, taking into account (13), gives

$$\frac{1}{\tau_0}\sum_v (P_{v0}\, n_0 - P_{0v}\, n_v) = \frac{1}{\tau_v}(n_0 - \theta_0 N)\,,$$

where τ_0 is the excimer free path time in the gas, and $P_{v'v}$ is the probability of transition from the vibrational level v to vibrational level v' in a single collision with a buffer gas atom (molecule), and, finally,

$$\tau_v = (1 - \theta_0)\tau_0\left(\sum_v P_{v0}\right)^{-1}.$$

Thus, the application of Eqn (2) is well-founded in the case of the Boltzmann distribution of molecules (13) over high vibrational levels which fail to contribute to light amplification.

Using k_{VT} parameters in level-to-level kinetic models requires consideration of the ambiguity in assessing kinetic parameters. This problem was discussed in Refs [23, 25] and lies in the fact that the same experimental data can be interpreted based on different sets of parameters of Eqns (4). Such a problem is always encountered whenever the number of independent variables exceeds that of equations containing these variables.

Now, let us calculate parameter k_{VT} of the diffusion equation (7). In the general theory of vibrational relaxation of diatomic molecules [43, 36], all information about their vibrational transitions is contained in the diffusion coefficient $B(\varepsilon)$. For multiquantum excimer transitions, $B(\varepsilon)$ must be derived from the relationship [70]

$$B(\varepsilon) = k_0[M]T\langle(\Delta\varepsilon)\rangle\,, \tag{14}$$

where $\langle(\Delta\varepsilon)\rangle$ is the average energy lost by a RgX(B, C) molecule in one collision with a buffer gas atom. At a buffer gas pressure $p \geqslant 0.1$ bar, collisional mixing between B and C states proceeds much faster than other relaxation processes, and $\langle(\Delta\varepsilon)\rangle$ should be calculated from the formula [70]

$$\langle(\Delta\varepsilon)\rangle = \frac{1}{2}\left[\sum_{v'} P_{v'v}^{BB}(\varepsilon_v - \varepsilon_{v'}) + \sum_{v'} P_{v'v}^{CC}(\varepsilon_v - \varepsilon_{v'}) + \sum_{v'} P_{v'v}^{BC}(\varepsilon_v - \varepsilon_{v'}) + \sum_{v'} P_{v'v}^{CB}(\varepsilon_v - \varepsilon_{v'})\right].$$

The quantity k_{VT} is determined using Eqn (14) and the approximation of $B(\varepsilon)$ by Eqn (8) in the region of low vibrational levels. Specifically, $\langle(\Delta\varepsilon)\rangle$ was calculated in Ref. [70] using probabilities (5) and (6) from Ref. [23]. The ε_v-dependence of $\langle(\Delta\varepsilon)\rangle$ thus obtained could be approximated by the linear function at $v = 16-60$, viz.

$$\langle(\Delta\varepsilon)\rangle = \frac{k_{VT}}{k_0}\,\varepsilon\,. \tag{15}$$

The vibrational relaxation rate constants derived from this relationship are presented in Table 4.

An indirect verification of k_{VT} values obtained from (15) was performed based on the vibrational relaxation theory for anharmonic oscillators [36]. According to this theory, the ε-dependence of the diffusion coefficient B in the case of non-

adiabatic collisions of the Morse oscillator with rare gas atoms is defined by the formula

$$B(\varepsilon) = \frac{2TD}{\tau_v}\sqrt{1-\frac{\varepsilon}{D}}\left(1-\sqrt{1-\frac{\varepsilon}{D}}\right),$$

where

$$\frac{1}{\tau_v} = \frac{4}{\tau_0}\frac{M_p}{\mu}\lambda_m^2,$$

D is the dissociation energy, M_p is the reduced mass of an atom and oscillator, μ is the reduced oscillator mass, and λ_m is the parameter depending on the atom to oscillator mass ratio. In the framework of this model, $k_{VT}(M)\mu/[k_0(M)M_p]$ must be independent of the kind of the inert gas M. According to the calculations performed in Ref. [70] for XeCl, the value of $k_{VT}\mu/(k_0 M_p)$ is 0.08 for He, Ar and 0.06 for Ne, Kr. Thus, the calculated values of $k_{VT}(M)\mu/[k_0(M)M_p]$ actually display a weak dependence on M.

Tables 2–4 show that one and the same term was applied to define the parameters of different kinetic equations. For this reason, it should be borne in mind, when using the constants k_{VT}, that different kinetic models are likely to provide different interpretations of the same experimental findings. This inference is illustrated by the following example.

4.2 Intensity of excimer lateral luminescence

In order to study active media of lasers, certain authors have observed the luminescence of electronically excited molecules in the direction perpendicular to the laser axis [7]. The patterns of this so-called lateral luminescence were first explained with the help of a phenomenological model of vibrational relaxation [21]. In the framework of this model, the formula was derived for the ratio of the luminescence intensity (I) of an electron band with and without laser generation:

$$\frac{I}{I_0} = \frac{N(\Phi)}{N(0)} = 1-\left(1-\frac{1}{\beta}\right)\frac{\Phi}{\Phi+\Phi_s'}. \qquad (16)$$

Here

$$\Phi_s' = \Phi_s\frac{1+\tau_u/\tau_v}{1+\theta_0\,\tau_u/\tau_v}, \qquad (17)$$

and $\Phi_s = h\nu/(\sigma\tau_u)$ is the saturant light flux found with the use of the simple two-level laser scheme [7, p. 46], and

$$\beta = 1+\theta_0\frac{\tau_u}{\tau_v}. \qquad (18)$$

The luminescence spectrum of XeF(B–X) shows lines corresponding to transitions from certain XeF(B) vibrational levels. Therefore, for the population ratio at the vibrational level with energy ε_0, the following formula was derived:

$$\frac{n_0(\Phi)}{n_0(0)} = 1-\left(1-\frac{1}{\beta_0}\right)\frac{\Phi}{\Phi+\Phi_s'}, \qquad (19)$$

which is analogous to (16). Here, β_0 is the parameter depending on the lifetimes of the upper and lower laser levels, their vibrational relaxation times, and population distributions [7, p. 376].

Formulae (16) and (19) were used many times in treating experimental data and later estimating the excimer laser efficiency. For example, I/I_0 was measured in active media of excimer KrF [21, 53], XeCl [49], and ArF [52] lasers, while $n_0(\Phi)/n_0(0)$ was measured in a XeF laser [85]. In accordance with (18), the parameter β exhibits a linear dependence on the vibrational relaxation rate constant k_{VT}. Therefore, this parameter was measured to assess the vibrational relaxation rate constants in the framework of phenomenological models [21, 53, 49, 52].

Formulae resembling (16) and (19) were also obtained with the help of the diffusion model of vibrational relaxation [70]. In this case, however, the dependence of Φ_s' and β on parameters of electronic-vibrational relaxation k_{VT}, τ_u turned out to be essentially different. That is, the saturant light flux Φ_s' was defined by the formulae presented in Table 5, whereas parameters β and β_0 were given by expressions

$$1-\frac{1}{\beta} = \eta_{st}\eta_l, \qquad 1-\frac{1}{\beta_0} = \eta_l.$$

Here, $\eta_{sp}(\varepsilon_0)$ and $\eta_{st}(\varepsilon_0)$ are the quantum yield of spontaneous emission and the ultimate quantum yield of stimulated emission from the vibrational level with energy ε_0, respectively. These parameters will be determined in the next section. Factor η_l takes into account stimulated phototransitions from a lower laser level to an upper one. The quantity η_l depends on τ (the effective time of depopulation of a lower laser level), τ_{ul} (the time of RgX transition from an upper to a lower laser level in consequence of spontaneous emission and radiationless deexcitation), and δ (the probability of I_2 transition from the upper electronic state D′ to a lower laser level [86]) (see Table 5). According to the diffusion model of vibrational relaxation, the quantity η_{st} is approximately equal to the parameter η^v (12), which may be estimated as $(T/\varepsilon^*)^{\tau_v/\tau_u}$ to an order of magnitude. Therefore, taking into account molecular distribution over vibrational levels leads to a more complicated dependence of β on k_{VT} and τ_u than follows from (18). Moreover, β shows a dependence not only on k_{VT}, τ_u and τ, but also on the energy of formation ε^* of electronically excited molecules.

Table 5. Parameters of formulae (16), (19), and (21)†.

Parameter	RgX(B → X) laser	I_2(D′ → A′) laser
$\frac{\Phi_s'}{\Phi_s}$	$\frac{\eta_{st}}{\eta_{sp}}\frac{\tau_u}{\tau_r}\left(1-\frac{\tau}{\tau_{ul}}+\frac{\tau}{\tau_r}\frac{\eta_{st}}{\eta_{sp}}\right)^{-1}$	$\frac{\eta_{st}}{\eta_{sp}}\frac{\tau_u}{\tau_r}\left(1+\frac{\tau}{\tau_r}\frac{\eta_{st}}{\eta_{sp}}\right)^{-1}$
η_l	$\left(1-\frac{\tau}{\tau_{ul}}\right)\left(1-\frac{\tau}{\tau_{ul}}+\frac{\tau}{\tau_r}\frac{\eta_{st}}{\eta_{sp}}\right)^{-1}$	$\left(1-\frac{\delta}{\tau_r}\frac{\tau}{\eta_{sp}}\right)\left(1+\frac{\tau}{\tau_r}\frac{\eta_{st}}{\eta_{sp}}\right)^{-1}$
$\frac{\gamma}{\gamma'}$	$1-\frac{\tau}{\tau_{ul}}$	$1-\frac{\delta}{\tau_r}\frac{\tau}{\eta_{sp}}$

† $\tau_r^{-1} \equiv (g_i/\sum_i g_i)A_{i-l}$, A_{i-l} is the Einstein coefficient for the transition between electronic states i and l, $\eta_{sp} \equiv \eta_{sp}(\varepsilon_0)$, and $\eta_{st} \equiv \eta_{st}(\varepsilon_0)$.

To summarize, the phenomenological [21] and diffusion [70] models offer similar formulae for the dependence of lateral luminescence intensities on the light flux Φ. However, the definitions of the saturant light flux Φ_s' and other parameters of Eqns (16) and (19) in Ref. [70] are essentially different from those generally accepted, (17) and (18) [7–10, 21, 22, 49–55].

5. Quantum yields of spontaneous and stimulated emission

The process of relaxation of electronically excited molecules from high to low vibrational levels is associated with the loss of a part of the excited molecules. This loss results, among other things, in a lower efficiency or the impossibility of light generation in the active media of lasers. Computation of the laser efficiency is therefore one of the most important applications of the theory. On the other hand, there is a wealth of data concerning excimer laser efficiency. These experimental findings can be employed in verifying theoretical approximations.

5.1 Quantum yield of spontaneous emission

Effect of vibrational relaxation on the efficiency of excimer lasers in the framework of the diffusion model was evaluated in a number of papers [63–66, 68–70]. In doing so Ref. [63] defines the quantum yield of spontaneous emission $\eta_{sp}(\varepsilon_v)$ as the ratio of the number of photons spontaneously emitted from the vth vibrational level of the ith electronic state to the number N of the molecules produced. The calculation of η_{sp} showed it to be of the same order of magnitude as the product of two cofactors, (τ_u/τ_r) and η^v.

The most important corollary of the theory is the predictable nonmonotone dependence of η_{sp} on the buffer gas pressure p. Indeed, the factor η^v exhibits a strong dependence on the parameter $\varkappa \equiv \tau_v/\tau_u$. Excimer quenching in collisions with two molecules (atoms) of the buffer gas M being neglected, the value of $\varkappa$ approximately equals

$$\frac{k_M}{k_{VT}} + \frac{1}{k_{VT}\tau_r}\frac{1}{[M]},$$

where k_M is the rate constant of excimer quenching by M particles, and τ_r is the radiative lifetime. This means that parameter $\varkappa$ decreases with growing [M], while the factor $\eta^v(\varkappa) \simeq (T/\varepsilon^*)^{\varkappa}$ increases until saturation at $[M] \gg (k_M\tau_r)^{-1}$. At the same time, another [M]-dependent cofactor, $\tau_u/\tau_r \simeq 1/(1 + k_M\tau_r[M])$, is a decreasing function of [M]. Hence, the nonmonotone p-dependence of the product of η^v and τ_u/τ_r comes to light. The predictable dependence of η_{sp} on the buffer gas pressure is illustrated in Fig 4. This figure shows $I_{sp}(p) = \eta_{sp}(p)R$, i.e. the intensity of spontaneous $I_2(D' - A')$ emission in gas mixtures excited by incoherent UV radiation at a pumping rate R which is independent of p. Commenting on the p-dependence of η_{sp}, it is appropriate to emphasize the importance of three-body quenching reactions with rates $k_M^M[M][M]$ for rare-gas halide excimers. In this case

$$\varkappa \simeq \frac{k_M}{k_{VT}} + (k_{VT}\tau_r)^{-1}\frac{1}{[M]} + \frac{k_M^M}{k_{VT}}[M],$$

hence, the factor η^v is a nonmonotone function of p.

5.2 Ultimate quantum yield of stimulated emission

An important laser characteristic is the ultimate quantum yield of stimulated emission η_{st}. This parameter was introduced as a maximally feasible ratio of the number of coherently emitted photons to that of the molecules produced [63, 64]. The ultimate quantum yield η_{st} corresponds to the saturation of the laser transition, a zero population of the lower laser level, and the absence of absorption in the active medium. The formula for η_{st} can be written as

$$\eta_{st}(\varepsilon_v) = \frac{\eta^v}{G(a, 1; \varepsilon_v/T)}, \qquad (20)$$

where G is a degenerate hypergeometric function of the second kind [88].

The ultimate quantum yields η_{sp} and η_{st} are of the same order of magnitude as η^v. However, η_{st} can be several-fold higher than η_{sp}. This property is illustrated by Fig. 5 in which $\eta_{st}(p)$ and $\eta_{sp}(p)$ correspond to the transition $I_2(D', v = 0 \to A')$ [64].

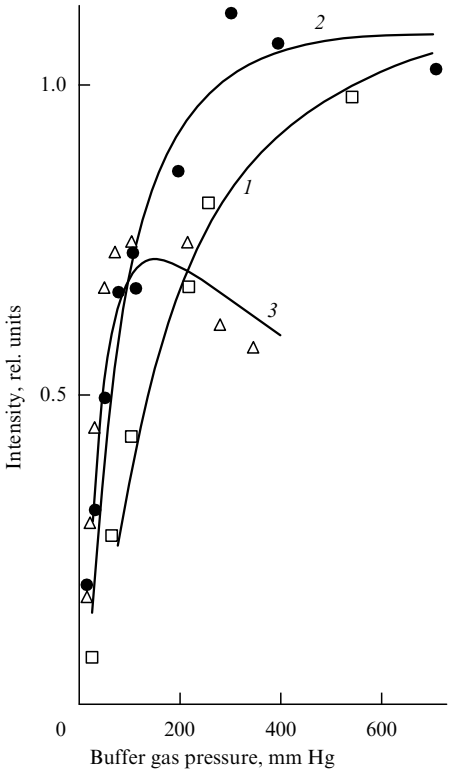

Figure 4. Computed (curves) [64] and observed (points) [87] dependences of spontaneous luminescence intensity $I_2(D' \to A')$ on the buffer gas pressure. Curve *1* and □ — CF_4, *2* and ● — C_3F_8, *3* and △ — C_5F_{12}.

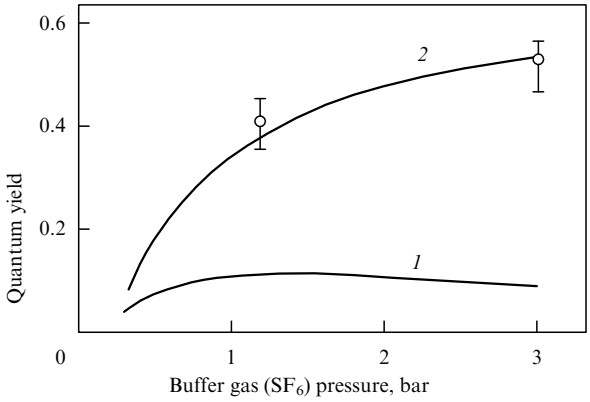

Figure 5. Quantum yields of spontaneous η_{sp} (curve *1*) and stimulated η_{st} (20) (curve *2*) emission for the $I_2(D', v = 0 \to A')$ transition. Experimental values correspond to the parameters of an $I_2(D' \to A')$ laser [89].

5.3 Quantum yield of excimer laser emission

In a recent study [70], a more detailed model was proposed for the vibrational relaxation of electronically excited molecules in the active media of electronic-transition molecular lasers. This model took into consideration the saturation of the gain coefficient and the finite time of laser lower level depopulation. The quantum yield of laser emission η was computed as the ratio of the specific number of laser photons leaving the resonator per second to the pumping rate for the excited molecules. The solution of the kinetic equation gave η in the form

$$\eta = \eta_{\rm st}(\varepsilon_0)\eta_{\rm l}\eta_{\rm em}\,. \tag{21}$$

Here

$$\eta_{\rm em} \equiv \frac{\Phi}{\Phi + \Phi_{\rm s}'} - \frac{1}{\gamma'}\,\frac{\Phi}{\Phi_{\rm s}'}\,.$$

Table 5 presents formulae for $\eta_{\rm l}$, $\Phi_{\rm s}'/\Phi_{\rm s}$ and γ'/γ, where γ is the ratio of the weak signal gain coefficient $g_0 = R\sigma A_{i-l}(g_i/\sum_i g_i)\eta_{\rm sp}$ to the light loss coefficient α.

Therefore, the quantum yield of emission may be presented as the product of three factors. The factor $\eta_{\rm st}$ takes into account effects of excitation, VT-relaxation, and quenching of molecules in an upper electronic state. The factor $\eta_{\rm em}$ is referred to as the quantum yield of the optical extraction and takes into account the dependence of η on Φ and γ. The factor $\eta_{\rm l}$ reflects stimulated phototransitions from the lower to higher laser level. Although the formula for $\eta_{\rm em}$ has a well-known form [7], the parameters $\Phi_{\rm s}'$ and γ' depend on the rate of electronic-vibrational relaxation in a higher electronic state and also on the population and depopulation kinetics of the lower laser level. $\Phi_{\rm s}'$ values were measured in a number of experiments.

It is worthwhile to note that in early studies, experimental data were treated using other definitions of the saturant light flux: $\Phi_{\rm s}' = \Phi_{\rm s}$ and (17). This qualitative difference is due to the preliminary assumptions about the molecular vibrational level distribution patterns in models [7, 21]. In fact, when only one level of the upper electronic state is populated, then $h\nu/(\sigma\tau_{\rm u})$ has to be used as $\Phi_{\rm s}'$. Formula (17) has been derived with the help of the phenomenological relaxation model [21]. In this model, changes of vibrational distributions in the region of high vibrational levels are disregarded (see the previous section).

It follows in particular from the formula for $\eta_{\rm em}$ that the optimal mirror reflection coefficient for the extraction of laser beam is characterized by

$$\Phi = \Phi_0 \equiv \Phi_{\rm s}'\left(\sqrt{\gamma'} - 1\right). \tag{22}$$

At $\Phi = \Phi_0$, the quantum yield η reaches its maximal value

$$\eta_{\max} = \eta_{\rm st}(\varepsilon_0)\eta_{\rm l}\left(1 - \frac{1}{\sqrt{\gamma'}}\right)^2. \tag{23}$$

These formulae were used to study the dependence of η on the depopulation time of the lower laser level [70]. Consideration of the effect of τ on η is of special importance for a XeF(B–X) laser. In such a system, the lower laser level presents a bound state with a dissociation energy $D \simeq 1200$ cm^{-1} [90]. Since the rate of XeF(X) dissociation grows with increasing T, the active medium of the laser has to be heated [85, 91–94]. This results in a rise of internal efficiency of the laser $\eta_{\rm int}$ related to η by the equality $\eta_{\rm int} = (h\nu/E)\,\eta$, where $h\nu$ is the energy of an emitted photon, and E is the energy expended on generating one electronically excited molecule (Table 6).

Table 6. Temperature dependence of the internal efficiency of a XeF laser at a gas pressure $p = 3$ bar.

Mixture	$\eta_{\rm int}$, % ($T = 300$ K)	T, K	$\eta_{\rm int}(T)$, %	$\frac{\eta_{\rm int}(T)}{\eta_{\rm int}(300\ {\rm K})}$	Ref.
NF_3–Xe–Ne	1.8	450	5.5	3.1	[91]
		500	5.2	2.9	
NF_3–Xe–Ne	—	500	—	1.5†	[85]
F_2–Xe–Ne	2.0 ± 0.1	450	3.5 ± 0.3	1.7	[93]
NF_3–Xe–Ne	2.0	450	3.2	1.6	[93]
NF_3–Xe–Ne	4.7	425	6.0	1.3	[94]
		475	5.7	1.2	

† Found from (19) by measuring the lateral luminescence intensity for the transition $B(v' = 0) \to X(v'' = 3)$ with $\lambda = 353$ nm.

In the majority of studies, the emission spectra of XeF lasers at $T = 300$ K show the most prominent line with $\lambda = 353$ nm corresponding to the transition $B, v' = 0 \to X, v'' = 3$. At $T \simeq 450$ K, the laser output energy is almost equally distributed between the line with $\lambda = 353$ nm and two lines corresponding to transitions $B, v' = 0 \to X, v'' = 2$ and $B, v' = 1 \to X, v'' = 4$ with $\lambda = 351$ nm. For this reason, in estimating η we can use the calculated [90] depopulation time of the XeF(X) fourth ($v'' = 3$) vibrational level for τ. It appears from the kinetic study [90] that the product of τ with the neon atomic concentration N is 4.5 ns atm at $T = 300$ K and 1.2 ns atm at $T = 450$ K.

Taken together, these $N\tau$ values and results of XeF laser studies [85] allow estimation of the parameter $\eta_{\rm l}$. It has been shown in Ref. [85] that the main reason for XeF(B) deexcitation is its interaction with electrons, and $\tau_{\rm u} = 3.8$ ns, $\tau_{\rm ul} = 4.4$ ns. The approximate equality $(\tau_{\rm r}/\tau_{\rm u})\,\eta_{\rm sp} \approx 0.8\eta_{\rm st}$ being fulfilled over a broad range of $\varkappa = 0.2-0.4$, one finds $\eta_{\rm l} = 0.65$ at $T = 300$ K. Taking into consideration only radiative transitions between the higher and lower laser levels, i.e. assuming $\tau_{\rm ul} = \tau_{\rm r} = 16$ ns, the calculation yields the same value, $\eta_{\rm l} = 0.57$. In other words, the efficiency of a XeF laser is impaired approximately two-fold at $T = 300$ K due to incomplete depopulation of its lower level.

The quantity $\eta_{\rm l}$ rises with increasing temperature of the active medium. For example, the calculation at $T = 450$ K for $\tau_{\rm ul} = 4.4$ ns gives $\eta_{\rm l}(450\ {\rm K})/\eta_{\rm l}(300\ {\rm K}) = 1.53$ (at $\tau_{\rm ul} = \tau_{\rm r}$, $\eta_{\rm l}(450\ {\rm K})/\eta_{\rm l}(300\ {\rm K}) = 1.36$). This rise in $\eta_{\rm l}$ agrees fairly well with the experimentally found temperature dependences of $\eta_{\rm int}$ (see Table 6). It is worthy of note that a rise in T alters not only $\eta_{\rm l}$ but also the absorption coefficient α of UV radiation [7]. Moreover, $\eta_{\rm st}$ also depends on T. In the model of interest, the characteristic time τ enters not only the formula for $\eta_{\rm l}$ but also defines Φ_0 (the light flux optimal for radiation extraction) and γ' [see Eqns (22), (23)]. This may in part account for a fall of $\eta_{\rm int}$ as T rises above 450 K in experiments with fixed R (see Table 6).

The formulae for $\eta_{\rm sp}$, $\eta_{\rm st}$ and η have been used in investigating active media of variety of excimer lasers. A theoretical study of $I_2(D' \to A')$ luminescence provided the parameters $k_{\rm VT}$ and $k_{\rm Q}$ for the $I_2(D')$ molecule [64], which were further used to calculate the quantum yield of stimulated emission in an $I_2(D' - A')$ laser. The optical properties of

KrF(B) excimer were evaluated in a similar way. In other studies, the efficiency of KrF lasers was estimated analytically [66, 68] and the gain coefficient in a KrF amplifier calculated [69]. The dependence of η on depopulation time of the lower laser level was illustrated by the temperature dependence of XeF laser efficiency [70].

An important feature of an excimer laser is a sharp decrease in the efficiency of populating low vibrational levels observed upon reduction of the buffer gas pressure p. This property is well apparent from Figs 4 and 5. Specifically, the diffusion model of vibrational relaxation predicts that the efficiency of upper level formation in a KrF(B–X) laser sharply decreases at a buffer gas pressure of around 0.1 bar. This conclusion is in agreement with recent measurements of the KrF(B–X) emission gain coefficient in Kr/F_2 mixtures excited either by an electron beam at $p = 50-200$ mbar [95] or by a longitudinal electric discharge at $p = 130-530$ bar [96].

Simplified models of excimer vibrational relaxation are well-described in numerous papers [7–10, 19, 21, 22, 49–55]. In these models, vibrational relaxation is taken into consideration by means of introducing an additional adjustable parameter k_{VT}. However, using this phenomenological approach for estimating the quantum yields of spontaneous and stimulated emission leads to the neglect of a number of important physical effects. Specifically, the simplified models fail to adequately describe the dependence of quantum yields of emission on the pressure, temperature, and gas composition. They cannot, in principle, describe various mechanisms of generating electronically excited molecules. In other words, it is sometimes crucial to model excimer relaxation kinetics with due regard for the consecutive population of a large number of vibrational states.

6. Electron-induced transitions in rare-gas halide excimers

6.1 Interaction between excimers and electrons

Formation of the active medium in an excimer laser is accompanied by the interaction between excimers and electrons of the plasma generated by an electric discharge or electron beam. Plasma electrons are involved in several relaxation processes, the principal one being excimer quenching by electron impact [97]:

$$e + \mathrm{RgX(B, C, D)} \xrightarrow{K_e} e + \mathrm{RgX(X, A, A')}\,. \qquad (24)$$

Quenching rate constants K_e for ArF^*, KrF^* and $XeCl^*$ were determined in experiments [98,49,99] to be of the order of 10^{-7} cm^3 s^{-1}. The calculated K_e values were obtained employing several theoretical models.

The order of magnitude of the rate constant K_e can be estimated using the Born approximation [100, 101, 2]. It gives an overestimated cross-section of inelastic electron scattering if the transition energy is comparable with the electron kinetic energy. Such an energy ratio does occur in the plasma of excimer lasers. For this reason, a more accurate calculation of electron scattering cross-sections for reaction (24) was undertaken [102] using a modified impact parameter method and electron wave functions of KrF and XeF molecules.

Based on the semiempirical computation of the cross-section of exciting optically allowed states by electron impact [103], the quenching rate constant was determined by the expression [97]

$$K_e = 1.1\,[\mathrm{cm}^{-1/2}]\,\frac{\lambda^{7/2}}{\tau_{nm}}\,, \qquad \frac{1}{\tau_{nm}} \equiv \frac{g_m}{g_n}\frac{f_{mn}8\pi^2e^2}{mc\lambda^2}\,. \qquad (25)$$

Here, λ, f_{mn} are the wavelength and the oscillator strength of the transition, respectively, and τ_{nm} is the lifetime. Expression (25) is applicable provided the electron kinetic energy is small compared with the transition energy. The K_e values calculated by different methods and obtained in experiments are correlated in Table 7. It can be seen from this table that the experimental and calculated values disagree. The discrepancy was accounted for by the existence of an additional quenching mechanism [97]. Studies [104, 105] concerned the formation of an electron–molecule bound state, followed by Penning ionization:

$$e + \mathrm{RgX}^* \leftrightarrow (\mathrm{RgX}^*)^-\,,$$
$$(\mathrm{RgX}^*)^- \rightarrow \mathrm{Rg} + \mathrm{X} + e\,. \qquad (26)$$

The formula given below was derived for the quenching rate constant in reactions (26) [97]:

$$K_e = \left(\frac{2\pi}{m}\right)^{3/2}\frac{\hbar\Gamma_1}{\sqrt{T}\,\omega}\exp\left(-\frac{U_0}{T}\right), \qquad (27)$$

where $\hbar\omega$ is the vibrational quantum of the autoionization state, U_0 is the excitation energy of the lower autoionization state, Γ_1 is the width of the autoionization level corresponding to its decay into an electron and RgX^*. By selecting the appropriate Γ_1 value, it is possible to establish a correspondence between experimental and theoretical K_e values.

A more precise analysis of experimental and theoretical findings was performed for the KrF^* excimer in Ref. [106]. It was concluded that the measured [98] and calculated [102] quenching rate constants of reaction (24) are virtually identical: $K_e(E/N) = (3-6) \times 10^{-8}$ cm^3 s^{-1}, where E/N is the electric field strength to particle concentration ratio.

In the active media of excimer lasers at XeF and XeCl transitions, electrons may play a positive role as well by accelerating the depopulation of the lower laser level in RgX(X) dissociation and vibrational relaxation reactions [107].

Plasma electrons markedly affect the vibrational distribution of stable molecules. This effect is apparent in salient features of active media kinetics. Specifically, taking into consideration the cascade population of HCl vibrational levels with $v = 0-3$ during collisions with electrons provided theoretical explanation of experimental data available for the XeCl laser [82, 108–113]. Similarly, an ArF laser model [114] took into account electron-induced vibrational excitation of F_2 and electron attachment to vibrationally excited F_2

Table 7. Rate constants of excimer quenching by electrons.

RgX	K_e, 10^{-8} cm^3 s^{-1}		
	Experimental data [98, 49, 99]	Calculations [102]	Calculated from (25)
ArF	23	—	0.9
KrF	20†	3†	1.1
XeF	40	7	1.8
XeCl	—	—	1.4

† A more accurate K_e lies in the range $(3-6) \times 10^{-8}$ cm^3 s^{-1} (see the text).

molecules. The effect of the dependence of the dissociative attachment rate constant on the degree of vibrational excitation leads to an attachment-vibrational instability of the discharge [115].

Apart from the quenching reactions (24), (26), electrons induce transitions between electronic and vibrational states in the RgX(B, C, D) molecules.

In the numerical XeCl-laser simulation [51], the vibrational relaxation of XeCl(B, C) excimers by electrons was taken into consideration. Specifically, the populations of XeCl(B) and XeCl(C) low-lying vibrational states were calculated with the aid of equations like (2), the right-hand sides of which contained terms of the form $-k_{\mathrm{Ve}} n_{\mathrm{e}}(n_0 - \theta_{\mathrm{e}} N)$, where n_{e} is the electron concentration, and

$$\theta_{\mathrm{e}} \equiv \exp\left(-\frac{\varepsilon_0}{T_{\mathrm{e}}}\right)\left[\sum_v \exp\left(-\frac{\varepsilon_v}{T_{\mathrm{e}}}\right)\right]^{-1}.$$

The adjustable parameter k_{Ve} was usually called the Ve-relaxation rate constant. The numerical value of $k_{\mathrm{Ve}}(\mathrm{XeCl}) = 5 \times 10^{-6}$ cm^3 s^{-1} was obtained by computing the luminescence intensity ratio of XeCl(B $\rightarrow$ X) to XeCl(C $\rightarrow$ A) measured in Ref. [49]. A similar approach was employed in modelling the vibrational relaxation of rare-gas halide excimers [56]. Comparison of experimentally [116–118] and theoretically [56] found quantum yields of excimer laser generation allowed the Ve-relaxation rate constants to be defined as $k_{\mathrm{Ve}}(\mathrm{KrF}) = (2-3) \times 10^{-7}$ cm^3 s^{-1}, and $k_{\mathrm{Ve}}(\mathrm{XeCl}) = 5 \times 10^{-7}$ cm^3 s^{-1}.

Analysis of electron effects on vibrational and electronic (B, C $\leftrightarrow$ D) transitions in RgX excimers was conducted in Ref. [71] using no adjustable parameters.

6.2 Effect of electrons on vibrational relaxation kinetics

The electron kinetic energy in an excimer laser plasma is much higher than the energy of the excimer vibrational transition $\hbar\omega_{mn}$. Therefore, the Bethe–Born approximation may be used to calculate the cross-section of inelastic electron scattering by molecules. With this approach, the rate constant of the transition from the m state with energy E_m to the n state with energy E_n will be proportional to the square of the transition dipole moment μ_{mn} [71]:

$$k_{mn} = \frac{16\sqrt{\pi}\,\mu_{mn}^2}{3a\sqrt{2T_{\mathrm{e}}m_{\mathrm{e}}}} \exp\left(\frac{E_m - E_n}{2T_{\mathrm{e}}}\right) K_O\left(\frac{|E_m - E_n|}{2T_{\mathrm{e}}}\right). \quad (28)$$

Here, a is the Bohr radius, m_{e} is the electron mass, and $K_O(x)$ is the modified Bessel function; also, it is assumed that the electrons have a Maxwellian velocity distribution with temperature T_{e}.

Formula (28) is applicable at low values of the Massey parameter $\delta = \omega_{mn} l/v$ [100], where l is the characteristic molecular size and v is the velocity of a particle striking a molecule. In an excimer laser plasma, the criterion $\delta \ll 1$ is satisfied for electrons. The calculation of δ for ion scattering under the same conditions yields $\delta \gg 1$. As a result, the effect of an ion on a molecule in excimer laser plasma resembles that of a corresponding neutral particle. It should be emphasized that formula (28) takes into account only the interaction between the electron and the molecular dipole moment. At present, the quadrupolar and polarization interactions are practically impossible to consider for the lack of necessary data. In principle, it is conceivable that the mechanism of vibrational relaxation in electronegative RgX molecules is triggered through the autoionization state of a negative $(\mathrm{RgX}^*)^-$ ion [97, 101].

Formula (28) allows the evaluation of the impact of plasma electrons on the kinetics of transitions with small energy transfer. Specifically, Eqn (28) was used to study the role of electrons in excimer vibrational relaxation kinetics.

Vibrational relaxation equation (7) is easy to generalize for the case when relaxation is caused by the collisions of molecules not only with buffer gas atoms (molecules) but also with electrons. Evidently, in this case, the particle flux

$$j = -B(\varepsilon, T)\rho(\varepsilon)\left(\frac{\partial}{\partial\varepsilon}\frac{f}{\rho} + \frac{f}{T\rho}\right)$$

in (7) should be substituted by $j + j_{\mathrm{e}}$, where

$$j_{\mathrm{e}} \equiv -k_{\mathrm{Ve}} n_{\mathrm{e}} T_{\mathrm{e}} \varepsilon\, \rho\left(\frac{\partial}{\partial\varepsilon}\frac{f}{\rho} + \frac{f}{T_{\mathrm{e}}\rho}\right), \quad (29)$$

and k_{Ve} is the rate constant of vibrational relaxation by electrons. In interactions between RgX^* excimers and electrons, the probabilities of forward ($v \rightarrow v-1$) and back ($v \leftarrow v-1$) transitions are very similar because T_{e} is much greater than the vibrational quantum $\hbar\omega$ of a molecule. In this case, k_{Ve} should be calculated using the expression [36, 43]

$$\frac{1}{2}\sum_n (\varepsilon_n - \varepsilon_m)^2 \mathrm{k}_{mn} = k_{\mathrm{Ve}} \varepsilon_m T_{\mathrm{e}} \qquad (\varepsilon_m \ll D). \quad (30)$$

By way of example, let us consider vibrational relaxation of a XeCl molecule by electrons. To begin with, the transitions between vibrational levels of a single electron state should be analyzed:

$$\mathrm{XeCl(B},v) + e \rightarrow \mathrm{XeCl(B},v \pm \Delta v) + e\,,$$
$$\mathrm{XeCl(C},v) + e \rightarrow \mathrm{XeCl(C},v \pm \Delta v) + e\,,$$

where $\Delta v = 1, 2, 3$. The μ_{mn} values necessary for the calculation were found in Ref. [71] using the theoretical approach described in Ref. [119]. For transitions between neighbouring XeCl(B, C) vibrational levels, $E_v - E_{v-1} = \hbar\omega \simeq 0.02$ eV and $\mu^2_{v,\,v-1} \simeq 0.2v\,\mathrm{D}^2$ (1 D $= 10^{-18}$ CGS units). For a typical value of $T_{\mathrm{e}} = 3$ eV, the rate constants of these transitions are $\mathrm{k}_{v,\,v-1} \simeq \mathrm{k}_{10} v$, where $\mathrm{k}_{10} \simeq 2 \times 10^{-8}$ cm^3 s^{-1}. The Ve-relaxation rate constant which is a parameter of formula (29) defined by expression (30), differs from k_{10}. The numerical value of K_{Ve} may be estimated through

$$k_{\mathrm{Ve}} \simeq \frac{\hbar\omega}{T_{\mathrm{e}}}\,\mathrm{k}_{10}\,. \quad (31)$$

In the example being considered, $k_{\mathrm{Ve}} = 2.5 \times 10^{-10}$ cm^3 s^{-1} for the electronic state C and 3.2×10^{-10} cm^3 s^{-1} for the state B of XeCl. For the collisionally mixed states B and C (at a buffer gas pressure $p \geqslant 0.1$ bar), one finds $k_{\mathrm{Ve}} = 2.9 \times 10^{-10}$ cm^3 s^{-1} [71].

Comparison of this rate constant with those derived when modelling XeCl luminescence shows that the adjustable parameters [56, 51] exceed the value from Ref. [71] by three and four orders of magnitude, respectively. Similar to the rate constants k_{VT} in Tables 2–4, the constants k_{Ve} are different due to their use in different kinetic models. The rate constant k_{Ve} from Ref. [71] must enter kinetic equation (7), while the constants k_{Ve} from Refs [56, 51] are equations of type (2).

Studies [56, 71] were designed to evaluate the role of electrons in excimer vibrational relaxation. Following [71], let us find the degree of plasma ionization $\alpha \equiv n_e/[M]$ at which the electron impact on vibrational relaxation kinetics can be neglected. In the framework of the diffusion model, the unknown values of α must be obviously defined by the condition

$$|j_e| \ll |j| , \tag{32}$$

where j_e is the electron flux (29), and j is the flux found without regard for electron effects.

In the region of high vibrational levels ($\varepsilon \gg T$), the distribution function (10) remains smooth and satisfies the approximate equality [63]

$$\frac{1}{f}\frac{df}{d\varepsilon} \simeq \frac{\varkappa - 1}{\varepsilon} .$$

As a result, inequality (32) takes the form $\alpha \ll k_{VT}/k_{Ve}$. In the region of low vibrational levels, it follows that

$$\frac{1}{f}\frac{df}{d\varepsilon} = -\frac{1}{T_v} ,$$

according to (10). Hence, a more rigorous condition for α must be met:

$$\alpha \ll \frac{T}{T_e}\frac{k_{VT}}{k_{Ve}} \simeq \frac{T}{\hbar\omega}\frac{k_{VT}}{k_{10}} . \tag{33}$$

The above data indicate that the k_{VT}/k_{Ve} ratio is of the order of 10^{-1} at $T/T_e \simeq 10^{-2}$. Normally, in excimer laser plasma $\alpha = 10^{-6}-10^{-5}$ [7]; therefore, criterion (33) is met. For this reason, plasma electrons have no appreciable effect on the kinetics of excimer vibrational relaxation.

However, it is worthwhile to note that in recent experiments [120,121] formation of excimers occurred in plasma with $\alpha \simeq 0.1$. Under these conditions, the rate of excimer vibrational relaxation by electrons was comparable with or even higher than the rate of excimer VT-relaxation by buffer gas atoms.

6.3 Transitions between B, C, and D states of RgX

The Bethe–Born approximation furnishing (28) was also employed to study the kinetics of electronic-vibrational transitions involving electronic B, C, and D states of RgX upon collisions between molecules and electrons. The $E_m - E_n$ and $\mu_{mn}^2 = \mu^2 q_{v'v''}$ quantities necessary to calculate k_{mn} [$q_{v'v''}$ is the Franck–Condon factor ($\sum_{v''} q_{v'v''} = 1$)] were found in Ref. [122] based on the data reported in Refs [119, 123]. The estimated values are shown in Table 8. In excimer laser active media, states B and C are collisionally coupled; therefore, for transitions from these states, one obtains $k_{B,C\to D} = (k_{B\to D} + k_{C\to D})/2$. Specifically, for a XeCl molecule, $k_{B,C\to D} \simeq 0.8 \times 10^{-8}$ cm^3 s^{-1} [71]. This theoretical value agrees with the experimental one [124].

Table 8. Excimer/electron interaction reactions.

RgX	Transition	$E_m - E_n$, eV	μ, D	q_{00}	k_{mn}, cm^3 s^{-1}
KrF	B, $v' = 0 \to$ D, $v'' = 0$	−0.73	0.59	0.82	1.1×10^{-8}
	C, $v' = 0 \to$ D, $v'' = 0$	−0.63	0.26	0.93	2.6×10^{-9}
XeF	B, $v' = 0 \to$ D, $v'' = 0$	−1.35	1.01	0.76	1.9×10^{-8}
	C, $v' = 0 \to$ D, $v'' = 0$	−1.30	0.48	0.75	4.5×10^{-9}
XeCl	B, $v' = 0 \to$ D, $v'' = 0$	−1.35	0.71	0.88	1.1×10^{-8}
	C, $v' = 0 \to$ D, $v'' = 0$	−1.28	0.31	0.88	2.2×10^{-9}

The rate constant $k_{B,C\to D}$ is used to estimate the effect of electrons on the D-state population in RgX excimers. The simplest kinetic model for the computation of populations N_1 in RgX(D) and N_2 in RgX(B, C) takes advantage of the following balance equations [124]:

$$\begin{aligned} &(A_1 + Q_1 + K_{12})N_1 - K_{21}N_2 = R_1 , \\ &-K_{12}N_1 + (A_2 + Q_2 + K_{21})N_2 = R_2 . \end{aligned} \tag{34}$$

Here, A_1 is the Einstein coefficient for the D → X transition; A_2 is the half-sum of the Einstein coefficients for transitions B → X and C → A; Q_1, Q_2 are the probabilities of radiationless deexcitation of RgX(D) and RgX(B, C) molecules per second; $K_{21} = k_{B,C\to D}\, n_e$ and $K_{12} = K_{21}\exp(\Delta E/T_e)$ ($\Delta E \equiv T_D - T_B$, $\Delta E = 1.3$ eV for RgX = XeCl) are the probabilities of forward and back transitions RgX(B, C) + $e \leftrightarrow$ RgX(D) + e, and, finally, R_1, R_2 are the population rates for RgX(D) and RgX(B, C), respectively. According to Eqn (34), one obtains

$$\frac{N_1}{N_2} = b\,\frac{A_2 + Q_2 + K_{21}(1 + 1/b)}{A_1 + Q_1 + K_{12}(1 + b)} , \tag{35}$$

where $b = R_1/R_2$ is the fraction of RgX molecules generated in the state D.

Equation (35) shows that plasma electrons of excimer lasers at typical n_e concentrations of order 10^{15} cm^{-3} [7, 124] induce a population of the RgX(D) state; in this case, the n_e-dependence of [RgX(D)] cannot be neglected at any b. For example, in an active medium [20] with electron concentration $n_e = (2-3) \times 10^{16}$ cm^{-3}, the concentration of KrF(D) was 15–20% of the [KrF(B)].

7. Vibrational distribution moments

7.1 Mean vibrational energy

An advantage of the analytical solution to the kinetic equation (7) is the simplicity of computing distribution function moments such as

$$\langle \varepsilon^n \rangle = \frac{\int_0^D d\varepsilon \int_{-\infty}^{\infty} dt\, \varepsilon^n f(\varepsilon, t)}{\int_0^D d\varepsilon \int_{-\infty}^{\infty} dt\, f(\varepsilon, t)} . \tag{36}$$

Indeed, it is sometimes necessary to know $\langle \varepsilon^n \rangle$ rather than the function $f(\varepsilon, t)$ itself since the numerical values of the first and second moments $\langle \varepsilon \rangle$ and $\langle \varepsilon^2 \rangle$ clearly indicate to what extent real vibrational distributions deviate from the equilibrium distribution.

In excimer vibrational relaxation studies, the ε-dependences of B and τ_u are as a rule unknown. However, it has been demonstrated that measured values normally exhibit a weak dependence on the specific shape of $B(\varepsilon)$ and $\tau_u(\varepsilon)$ [65, 69]. This makes it possible to neglect the ε-dependences of τ_u and ρ and approximate $B(\varepsilon)$ with the linear function (8). The use of these approximations allows the analytical solution of the Fokker–Planck equation to be found in the form of an

expansion in Laguerre polynomials:

$$f(\varepsilon, t) = \exp\left(-\frac{\varepsilon}{T}\right) \sum_n a_n(t) L_n\left(\frac{\varepsilon}{T}\right).$$

Moments $\langle\varepsilon\rangle$ and $\langle\varepsilon^2\rangle$ will be expressed through the expansion coefficients a_2 and a_1. Specifically, for the pumping rate

$$r(\varepsilon, t) = \frac{N_0}{\sqrt{2\pi}\, t_e} \exp\left[-\frac{1}{2}\left(\frac{t}{t_e}\right)^2\right] \delta(\varepsilon - \varepsilon^*), \tag{37}$$

it follows [72] that

$$\langle\varepsilon\rangle = \frac{\varkappa\varepsilon^* + T}{1+\varkappa}, \qquad \langle\varepsilon^2\rangle = \frac{\varkappa(\varepsilon^*)^2}{2+\varkappa} + \frac{4(\varkappa\varepsilon^* + T)T}{(2+\varkappa)(1+\varkappa)}. \tag{38}$$

Let us compare these moments with the corresponding characteristics of the high-temperature Boltzmann distribution

$$f_B(\varepsilon) = \frac{N}{T_v} \exp\left(-\frac{\varepsilon}{T_v}\right). \tag{39}$$

The computation of the mean ε^n by (39) gives

$$\langle\varepsilon\rangle_0 = T_v, \qquad \langle\varepsilon^2\rangle_0 = 2T_v^2. \tag{40}$$

The values of $\langle\varepsilon\rangle$ defined by the formulae (40) and (38) frequently differ from each other by an order of magnitude. This difference is illustrated by the following estimates. In a recent experiment [59], the pulse formation of XeCl(B, C) molecules with a vibrational energy of $\varepsilon^* \simeq 1.2$ eV was observed. Evaluating the contribution of selected vibrational levels with $v = 0-5$ to the time-averaged XeCl($B \to X$) luminescence spectrum allowed a determination of $T_v = 500$ K. It should be noted that the real distribution (10) has the same shape as the Boltzmann distribution (39), but formula (10) is applicable over a narrow range of ε. If parameter T_v is known, formula (11) may also be used to derive the τ_v/τ_u value. In the example being examined, $\varkappa = 0.4$. Furthermore, it follows from (38) that $\langle\varepsilon\rangle = 0.34$ eV. This value of $\langle\varepsilon\rangle$ is 8 times that of the measured vibrational temperature $T_v = 500$ K and $\langle\varepsilon\rangle_0$.

Even higher $\langle\varepsilon\rangle$ values are characteristic of excimers formed in the active media of excimer lasers. In fact, excimer laser active media are excited either by an electron beam or electric discharge. With this pumping mode, RgX molecules are largely formed near the dissociation limit with $\varepsilon^* \simeq D \simeq 4-5$ eV. For a characteristic value of $\varkappa = 0.3$, $\langle\varepsilon\rangle \simeq 1$ eV. Therefore, the calculation of $\langle\varepsilon\rangle$ indicates that, in reality, a significant part of the excimers populate high vibrational levels.

7.2 Vibrational distribution dynamics in the case of pulse excitation

Let us now examine the vibrational distribution dynamics under pulse excitation of high vibrational levels in more detail. To this effect, it is necessary to analyze the results of calculating [67, 72] time-dependent moments

$$\overline{\varepsilon^n}(t) = \frac{\int_0^D \varepsilon^n f(\varepsilon, t)\, d\varepsilon}{\int_0^D f(\varepsilon, t)\, d\varepsilon}. \tag{41}$$

Using the same approximations as in Section 7.1, it is easy to find for the pumping rate

$$r(\varepsilon, t) = \frac{N_0}{\sqrt{2\pi}\,\Delta_0} \exp\left[-\frac{1}{2}\left(\frac{\varepsilon - \varepsilon^*}{\Delta_0}\right)^2\right] \delta(t)$$

that

$$\overline{\varepsilon}(t) = T(1-z) + \varepsilon^* z,$$
$$\overline{\varepsilon^2} - (\overline{\varepsilon})^2 \equiv \Delta(t) = T^2(1-z)^2 + 2T\varepsilon^*(1-z)z + \Delta_0^2 z^2, \tag{42}$$

where $z \equiv \exp(-t/\tau_v)$. At $t = 0$, formulae (42) correspond to the initial distribution parameters $\overline{\varepsilon} = \varepsilon^*$ and $\Delta = \Delta_0$. At $t = t_m \equiv \tau_v \ln(\varepsilon^*/T)$ and $\varepsilon^* \gg T$, $\varepsilon^* \gg \Delta_0$, we have $\overline{\varepsilon} = 2T$ and $\Delta = \sqrt{3}\, T$. The value of $\overline{\varepsilon}$ thus found is only twice the equilibrium value, i.e. T. At $t = 2t_m$, the deviation of $\overline{\varepsilon} = T(1 + T/\varepsilon^*)$ from T may be neglected. In other words, in the course of time, molecules in the electronically excited state achieve the Boltzmann vibrational distribution with $T_v = T$. The relaxation dynamics of the vibrational distribution is illustrated in Fig. 6.

Taken together, the above estimates and Fig. 6 make it possible to estimate the characteristic time necessary for vibrational equilibrium to be established under pulse pumping. Evidently, it equals t_m. Let us compare this quantity with other characteristics of the vibrational relaxation process.

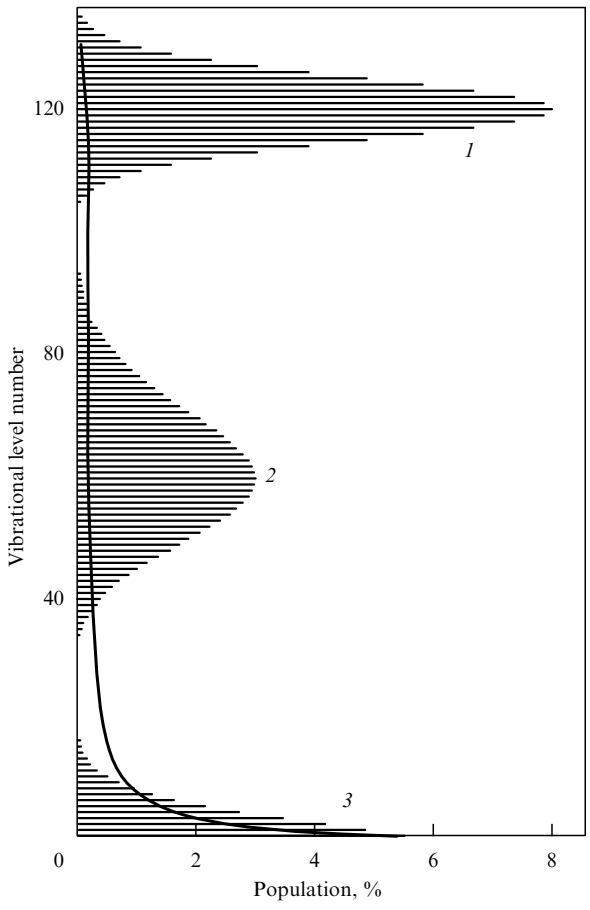

Figure 6. Nonstationary vibrational distributions computed for $\varepsilon^* = 120\,\hbar\omega$, $T = \hbar\omega$ and $\tau_v = 0.3\tau_u$. Diagram *1* corresponds to $t = 0$, *2* to $t = \tau_v \ln 2$, and *3* to $t = \tau_v \ln(\varepsilon^*/T)$. The solid line is the envelope for time-integrated populations $\int_0^\infty n_v(t)\, dt/(2\tau_u)$.

The objective of a KrF(B–X) laser study [69] was to examine, among other parameters, the time-dependent characteristics of the gain coefficient $g(t)$. A salient feature of KrF excimers is that a few vibrational levels of the electronic state B contribute to the light emission with $\lambda = 248$ nm. For this reason, the gain coefficient is expressed through the sum

$$g(t) = \frac{\sigma}{\hbar\omega} \sum_{v=0}^{2} f(\varepsilon_v, t) .$$

In Ref. [69], a delay between pumping (37) and gain (Fig. 7) pulses was found to equal

$$t_d = \langle t \rangle = \tau_u + \tau_v \ln \frac{\varepsilon^*}{\varepsilon'} ,$$

where $\varepsilon' = 3\hbar\omega$, and

$$\langle t^n \rangle = \frac{\int_{-\infty}^{\infty} t^n g(t)\, dt}{\int_{-\infty}^{\infty} g(t)\, dt} .$$

Moreover, the luminescence pulse length t_b was calculated to be

$$t_b^2 = \langle t^2 \rangle - \langle t \rangle^2 = t_e^2 + \tau_u^2 .$$

The value characterizing $g(t)$ asymmetry, $\langle (t - \langle t \rangle)^3 \rangle = 2\tau_u^3$, was obtained in a similar manner. Comparing the formulae for t_d and t_b shows that the function $g(t)$ has a maximum at $t \simeq t_m$.

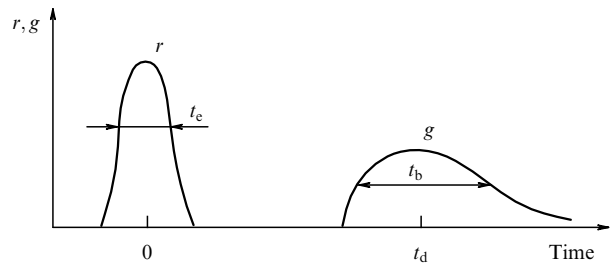

Figure 7. Comparison of KrF excimer excitation and amplification pulses.

In addition to the KrF(B–X) laser, the luminescence of other molecules was also studied. For example, Refs [67, 72] report the luminescence intensity I_v for the radiative transition from the vth vibrational level. According to these findings, to be discussed in more detail in the next section, the function $I_0(t)$ has the maximum at

$$t_{max} = \tau_v \left(\ln \frac{\varepsilon^*}{T} + \ln \frac{\tau_u}{\tau_v} \right) , \qquad (43)$$

when excimers are excited by a short pumping pulse. Formula (43) is applicable at $\varepsilon^* \gg T$.

Thus, the pulse luminescence intensity $I_v(t)$ for transitions from low vibrational levels peaks at $t \simeq \tau_v \ln(\varepsilon^*/T)$ ($\varepsilon^* \gg T$). It has been mentioned above that at this point in time the $\bar{\varepsilon}$ value obtained from (42) is approximately twice as large as T and much smaller than the time-averaged vibrational energy $\langle \varepsilon \rangle$ determined by (38).

This inference is interesting to compare with experimental findings. Thus, Ref. [59] reports the excitation of a Cl_2/Xe mixture with a partial pressure of 100 mm Hg by a light pulse as long as $t_e = 6-8$ ns. As noted above, the vibrational temperature T_v was determined from the time-averaged luminescence spectrum of XeCl(B → X). Time-averaging was performed for three time intervals: 0–30 ns, 30–150 ns, and 0–150 ns. The calculation of τ_u for the said gas mixture using kinetic parameters [59] yielded $\tau_u = 14$ ns. Therefore, we obtain $\tau_v = 6$ ns at $\varkappa = 0.4$, while $t_{max} = 27$ ns, in accordance with (43). The computed point in time $t \simeq 30$ ns at which the luminescence intensity $I_0(t)$ is highest, agrees fairly well with the measured value [59]. For the time of the luminescence spectrum averaging between 0 and 30 ns, the observed temperature T_v was in excess of 500 K but below 800 K. It was approximately 300 K but lower than 500 K for the averaging time from 30 to 150 ns. The mean temperature T_v (for $t = 0-150$ ns) was equal to 500 K. At $t = t_{max}$, $\bar{\varepsilon} = 420$ K, according to Eqns (11) and (42). Thus, the formula for $\bar{\varepsilon}(t)$ is consistent with the dynamics of the XeCl(B) distribution over low vibrational levels observed in Ref. [59].

8. Some applications of the diffusion model

8.1 Pulse luminescence kinetics

The diffusion model of vibrational relaxation was used not only to determine $\langle \varepsilon^n \rangle$, $\overline{\varepsilon^n}(t)$ and $\langle t^n \rangle$, but also to directly compute the luminescence intensity of excimers. For example, the authors of Ref. [67] investigated $I_2(D' \to A')$ pulse luminescence arising from subnanosecond excitation of an I_2/Ar mixture [47]. A simple analytical solution of Eqn (7) [67] was found with coefficient (8), constant τ_u and ρ, and

$$r(\varepsilon, t) = N_0\, \delta(\varepsilon - \varepsilon^*)\, \delta(t) . \qquad (44)$$

In particular, the distribution function $f(\varepsilon)$ at $\varepsilon < T$ was approximated by the function

$$f(0, t) = \frac{N}{T} z^{\varkappa} (1 - z)^{-1} \exp\left(-\frac{\varepsilon^*}{T} \frac{z}{1 - z} \right) , \qquad (45)$$

where $z \equiv \exp(-t/\tau_v)$.

The analytical solution of the Fokker–Planck equation provided an explanation for the results of an experiment in which $I_2(D' \to A')$ luminescence was observed at two wavelengths, $\lambda_1 = 342$ and $\lambda_2 = 323$ nm, and at different buffer gas pressures (150, 300, and 700 mm Hg). Figure 8 shows the $I_v(t)$ dependence for $v = 0$ (transition with λ_1) and $v = 9$ (transition with λ_2) [48], while Fig. 9 presents the dependence of $I_0(t)$ estimated and measured at an argon pressure of 150, 300, and 700 mm Hg. It follows from Figs 8 and 9 that the theoretical and experimental dependences are in good agreement at $t < 30$ ns.

The calculations reported in Ref. [67] made use of the following set of parameters: $k_{VT} = 2 \times 10^{-11}$ cm^3 s^{-1}, $\tau_u = \tau_r = 6.7$ ns, $\varepsilon^* = 0.5$ eV, where τ_r is the effective radiative lifetime. This set was deduced from the comparison of theoretical and experimental $I_v(t)$ dependences. Moreover, the same values of parameters were used earlier for calculating the $I_2(D' \to A')$ luminescence quantum yield [64].

It can be seen from Fig. 9 that the concord between theoretical and experimental $I_0(t)$ curves is not so good at $t > 30$ ns. This discrepancy can be accounted for by the use of

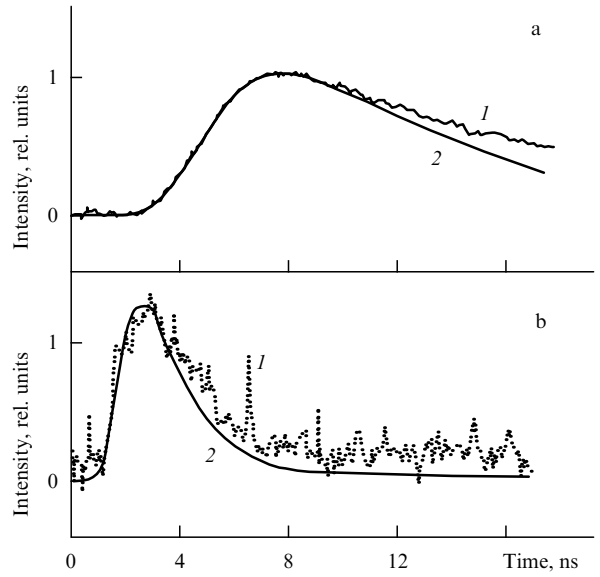

Figure 8. Time dependence of the luminescence intensity for transitions from $I_2(D', v = 0)$ with $\lambda = 342$ nm (a) and $I_2(D', v = 9)$ with $\lambda = 323$ nm (b) at a buffer gas pressure of 700 mm Hg. Curve *1* shows the experimental dependence [47]; curve *2* is calculated using the diffusive relaxation model [67].

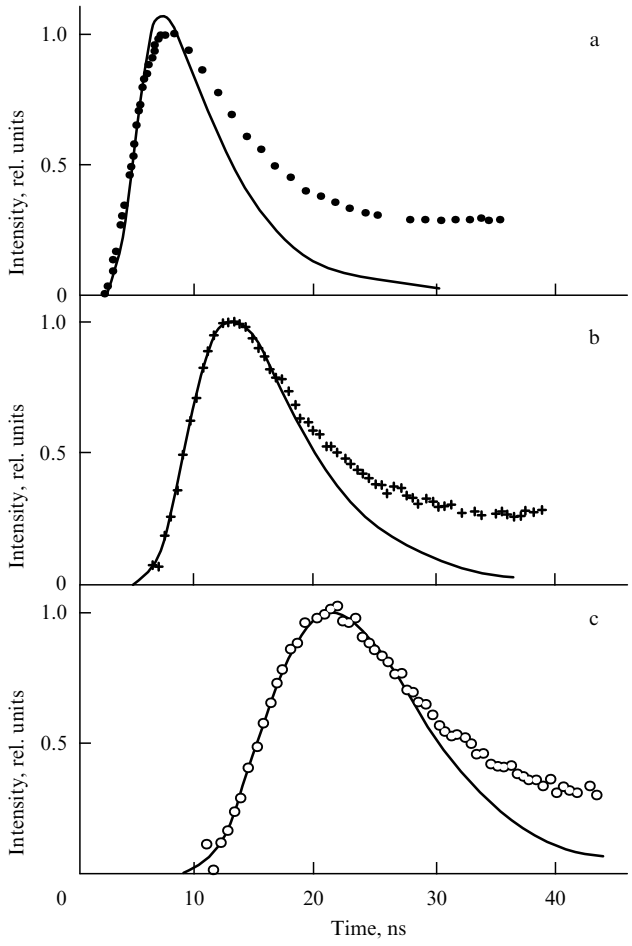

Figure 9. Luminescence intensity of the $I_2(D', v = 0)$ transition with $\lambda = 342$ nm as a function of time. The Ar pressure was set at the following values: (a) 700 mm Hg, (b) 300 mm Hg, (c) 150 mm Hg. The points denote experimental values, while the solid lines were calculated from formula (45) [67].

formula (44), which describes the formation of I_2^* in the reactions of electrons with $I_2(X)$ molecules. In other words, slower processes of energy transfer from the excited Ar^* atoms and Ar_2^* molecules to $I_2(X)$ as well as the ion – ion recombination processes were disregarded [125].

Formula (45) allows for the comparison of pulse luminescence dynamics predicted by different kinetic models. The phenomenological approach described in Sections 2.1 and 4.2 was frequently used in modelling excimer kinetics. In a simplified kinetic model [21], the population n_0 of the ground vibrational level is derived from Eqns (2) and (3). It follows from these equations that in the case of instantaneous formation of vibrationally excited N_0 molecules $[R = N_0\,\delta(t)]$ the population n_0 must be changing in accordance with the law

$$n_0 = N_0\theta_0 z^{\varkappa}(1 - z)\,, \tag{46}$$

where $\varkappa \equiv \tau_v/\tau_u$.

In the diffusion model of vibrational relaxation, it follows from (45) that

$$n_0 = N_0\,\frac{g_i}{\sum_i g_i}\,\frac{\hbar\omega}{T}\,z^{\varkappa}(1 - z)^{-1}\exp\left(-\frac{\varepsilon^*}{T}\,\frac{z}{1 - z}\right). \tag{47}$$

Let us compare (46) and (47) on the assumption that parameters τ_v and τ_u are identical in the simplified and diffusion models, and $\varepsilon^* \gg T$. Function (46) has the maximum at $t = t_{max}$, where

$$t_{max} = \tau_v\,\ln\left(\frac{\tau_u}{\tau_v} + 1\right). \tag{48}$$

The maximum of function (47) is reached later [cf. (43)]. Accordingly, it will be $(\varepsilon^*/T)^{\varkappa}$ times smaller than the maximum of (46). Therefore, the model taking into account the nonequilibrium population of many vibrational levels predicts substantially heavier relaxation losses of excited molecules. For instance, at $\tau_v = \tau_u$, one finds $n_0(t_{max}) \simeq (1/4)N_0$ in accordance with Eqns (46) and (48), whereas Eqns (47) and (43) predict $n_0(t_{max})$ to be of order $(T/\varepsilon^*)N_0$ (the T/ε^* ratio is usually close to 0.01).

8.2 Dynamics of the gain recovery in active media of excimer lasers

Peculiarities of the vibrational relaxation kinetics of electronically excited molecules make themselves evident in the dynamics of the gain coefficient $g(t)$ in excimer lasers. The $g(t)$ dynamics was first minutely examined in a XeCl excimer amplifier [26]. These experiments demonstrated the recovery of g following the passage of a saturant picosecond light pulse through the active medium. It was also discovered that at $t > 0.2$ ns the gain coefficient varies according to

$$g(t) = g_0 - \Delta g\exp\left(-\frac{t}{\tau_s}\right), \tag{49}$$

where the parameter $\tau = 2.5$ ns was referred to as the energy storage time. Here, time $t = 0$ corresponds to the passage of the saturating pulse. At $0 < t < 0.2$ ns, the recovery of g depends on rotational relaxation and collisional mixing of XeCl(B) and XeCl(C) molecules and also on XeCl(X) dissociation [26, 27].

A theoretical examination of $g(t)$ nanosecond dynamics was undertaken using a diffusion model of vibrational relaxation [67]. In the case of steady-state pumping of high vibrational levels, the instantaneous deexcitation of ΔN molecules populating the vibrational level with energy ε_0 was simulated by the function

$$r(\varepsilon, t) = r_0(\varepsilon) - \Delta N \delta(\varepsilon - \varepsilon_0)\, \delta(t)\,.$$

The analytical solution of the Fokker–Planck equation for such an $r(\varepsilon, t)$ dependence was found to be [67]

$$f(\varepsilon, t) = f_0(\varepsilon) - \frac{\Delta N}{T} \exp\left(-\frac{\varepsilon}{T}\right) \exp\left(-\frac{t}{\tau_u}\right) \times \sum_{n=0}^{\infty} \exp\left(-n\,\frac{t}{\tau_v}\right) L_n\left(\frac{\varepsilon_0}{T}\right) L_n\left(\frac{\varepsilon}{T}\right), \quad (50)$$

where f_0 is the stationary distribution function. In the case of zero population of a lower XeCl-laser level, the gain coefficient can be defined as $g(t) = \sigma f(\varepsilon_0, t)\hbar\omega$, where $\varepsilon_0 = 0.5T$ for the ground vibrational level of a XeCl(B) excimer [26]. It follows from Eqn (50) that the function $g(t)$ is practically independent of τ_v at $t \geqslant \tau_v$ and equality (49) is fulfilled, where $\tau_s = \tau_u$ and $\Delta g = \sigma \Delta N(\hbar\omega/T)\exp(-\varepsilon_0/T)$.

Therefore, the recovery time τ_s of the gain coefficient is close to the quenching time τ_u for electronically excited molecules.

This inference is in agreement with the results of measuring $g(t)$ (49). Indeed, for a mixture with partial pressures of HCl, Xe and Ne equal to 3, 15 and 5 mm Hg, respectively, and an electron concentration of 9×10^{14} cm^{-3}, the recovery time τ_s of the gain coefficient turned out to be 2.5 ns. Calculations of τ_u using a theoretical model of a XeCl laser [99] yield a similar value of 2.4 ns.

9. Amplification of far IR radiation by rare gas halides

An important corollary to the vibrational relaxation theory is the nonequilibrium population of high vibrational levels, confirmed by a wealth of experimental data. This property of excimers provided the basis for the theoretical prediction of a new physical phenomenon [126]. Namely, it has been shown (1) that population inversion for certain vibration–rotation levels of excimer species does exist, and (2) that laser IR generation is feasible in the active media of excimer lasers.

9.1 Criteria for population inversion in vibration–rotation transitions

Let us consider the excimer distribution over vibrational energy in the region of high vibrational levels. The following stationary distribution function was found for the pumping rate of type $r = R\delta(\varepsilon - \varepsilon^*)$ with regard for vibrational anharmonism [63]:

$$f_0(\varepsilon) = R\tau_v \frac{\hbar\omega}{2D} \frac{\left[1 - (1 - \varepsilon/D)^{1/2}\right]^{\varkappa - 1}}{\left[1 - (1 - \varepsilon^*/D)^{1/2}\right]^{\varkappa}} \rho(\varepsilon)\,, \quad (51)$$

where $\rho(\varepsilon)$ is the density of vibrational states for the Morse oscillator. In an atmosphere of light inert gases, the characteristic value of τ_v is $10^2\tau_0$, where τ_0 is the excimer free path time in the gas. At the same time, the rotational relaxation time τ_{RT} is of order τ_0 [26, 127, 75, 27, 128, 129, 76, 46]. Therefore, the conditions

$$\tau_{RT} \ll \tau_u\,, \qquad \tau_{RT} \ll v^{-1}\tau_v \quad (52)$$

being satisfied, the excimer distribution over rotational levels will be of Boltzmann type with gaseous temperature T.

The inequalities (52) impose constraints on the rare gas pressure and the vibrational quantum number v. They being met, the inversion density at the vibration–rotation transition $v, j \to v - 1, j \pm 1$ is given as

$$\Delta^{v,j}_{v-1,j\pm1} = \left(\pm\frac{j}{j^2_{max}} - \frac{1-\varkappa}{v}\right) \frac{(2j+1)B}{T} \exp\left[-\frac{j(j+1)}{T}\right] \frac{f(\varepsilon_v)}{\rho(\varepsilon_v)}\,, \quad (53)$$

where B is the excimer rotational constant, ε_v is the energy of the vth vibrational level, and $j_{max} = (2B/T)^{-1/2}$ is the number of the maximally populated rotational level. Full inversion occurs at $\varkappa > 1$ [130]. Light amplification is possible for all transitions within P-branches of the vibration–rotation spectrum and those transitions within R-branches for which $j < j^2_{max}(\varkappa - 1)/v$. At $\varkappa < 1$, a partial inversion occurs, and light amplification is likely only for P-branch transitions with $j^2_{max}(1 - \varkappa)/v < j < j^2_{max}\hbar\omega/T$ [126].

9.2 Coefficients of light amplification by RgX excimers in the far IR spectral region

The gain coefficient by the $v, j \to v - 1, j \pm 1$ transition is routinely expressed through the matrix element of the dipole moment of the $v \to v - 1$ transition [130]. It is well-known that rare-gas halide excimers possess ionic bonds. The dipole moments of such molecules exhibit an approximately linear dependence on the internuclear distance. For this reason, optical transitions between neighbouring vibrational levels in rare gas halides are allowed. In order to calculate the cross-section $\sigma_{v,j}$ of stimulated IR radiation it is necessary to know the dependence of the molecular dipole moment on the internuclear distance. This dependence was calculated for RgF molecules, where Rg = Ne, Ar, Kr, Xe, and XeX molecules in which X = F, Cl, Br, I [119, 123]. The collisional width of the IR radiation line may be assumed to be 4 GHz atm^{-1} [127]. The calculated parameters of IR transitions for selected excimers are presented in Table 9 [126]. In this table, λ is the radiation wavelength corresponding to transitions from $v = 10$ up to $v = 50$, A_1 is the Einstein coefficient for the transition $v = 1 \to v = 0$, and p is the buffer gas pressure reported in atmospheres.

Table 9. Parameters of excimers showing optical activity in the IR spectral region.

Excimer	KrF	XeF	XeCl
λ, μm	35–50	35–60	55–70
A_1, s^{-1}	0.8	0.9	0.2
$\sigma_{1,j_{max}}\,p$, 10^{-16} cm^2 atm^{-1}	0.5	0.6	0.3

The gain coefficient for IR radiation is expressed through the inversion density

$$\alpha^{v,j}_{v-1,j\pm1} = \sigma_{v,j}\Delta^{v,j}_{v-1,j\pm1}$$

and depends on the excimer generation rate R. The gain coefficient can also be expressed through the excimer concentration $N = \int_0^D f_0(\varepsilon)\,d\varepsilon$. For transitions from a maxi-

mally populated rotational level, it follows that

$$\alpha_{v-1,j_{\max}\pm1}^{v,j_{\max}} = \left(\pm\frac{1}{j_{\max}} - \frac{1-\varkappa}{v}\right)\left(\frac{\varkappa}{\sqrt{e}\,j_{\max}v}\right)\left(\frac{\varepsilon_v}{\varepsilon^*}\right)^{\varkappa} N,$$

according to Eqns (53) and (51).

The N values can be deduced from experimentally examined spontaneous UV radiation powers. In one such study, a mixture of $F_2 : Kr : He = 2 : 5 : 100$ was excited in a 3 cm^3 cell by a longitudinal electric discharge at $p = 0.05$ atm and $T = 300$ K [131]. The total energy of spontaneous UV radiation of KrF was 32 mJ at an emission pulse length around 100 ns. Hence, the total excimer concentration constituted approximately 3×10^{15} cm^{-3}. In the active medium of interest, $\varkappa \simeq 1$, $\varepsilon^* \simeq 1.8$ eV, and the first criterion in (52) is met. For a KrF(B) excimer at the vibration–rotation transition $v = 25, j_{\max} = 22 \to v = 24, j = 23$ with a radiation wavelength $\lambda = 40$ μm, one finds $\alpha = 2 \times 10^{-3}$ cm^{-1}. For the transition $v = 50, j_{\max} = 22 \to v = 49, j = 23$ with $\lambda = 50$ μm, $\alpha = 4 \times 10^{-3}$ cm^{-1}. The absorption coefficient for IR radiation by plasma electrons at a concentration of 10^{-14} cm^{-3} is close to 10^{-4} cm^{-1} [132], i.e. it is an order of magnitude smaller than the gain coefficient under the same conditions.

To summarize, the active media of excimer lasers allow for the amplification of both UV and IR radiation. In compliance with the vibrational relaxation theory, population inversion and amplification of IR radiation occur in many vibration–rotation transitions. Due to RgX vibrational anharmonism, the effect must be apparent over a broad range of light wavelengths from 30 to 50 μm.

10. Electronic relaxation parameters of excimers

10.1 Electronic relaxation equation

As a rule, electronic relaxation of excimers is described by an integral equation for the total particle concentration. This equation represents in fact the vibrational relaxation equation (7) integrated over ε:

$$\frac{\mathrm{d}N}{\mathrm{d}t} = R - \frac{1}{\tau_{\mathrm{re}}} N - \sum_{\mathrm{Q}} K_{\mathrm{Q}}[\mathrm{Q}]\, N - \sum_{\mathrm{Q,M}} K_{\mathrm{Q}}^{\mathrm{M}}[\mathrm{Q}][\mathrm{M}]N. \quad (54)$$

Here, $N = \int f(\varepsilon, t)\,\mathrm{d}\varepsilon$ is the excimer concentration and $R = \int r(\varepsilon, t)\,\mathrm{d}\varepsilon$ is the total pumping rate. The parameters of Eqn (54) are the effective radiative lifetime $\tau_{\mathrm{re}} = \sum_i g_i / \sum_{i,l} g_i \langle A_{i-l}\rangle$ and the rate constants $K_{\mathrm{Q}} = \langle k_{\mathrm{Q}}(\varepsilon)\rangle$, where $k_{\mathrm{Q}}(\varepsilon)$ is the rate constant of deexcitation of an excimer with an energy ε during collisions with the particle Q. We shall use the notation $\langle \ldots \rangle$ with the same meaning as in the definition of (41), which coincides with (36) in the case of a quasi-stationary excimer formation. K_{Q} values are normally obtained by measuring luminescence quenching. Therefore, K_{Q} is called the quenching rate constant of electronically excited molecules.

10.2 Variation of kinetic parameters

Measurements of one and the same kinetic parameter may yield significantly different results. For example, the following rate constants of XeCl excimer quenching by HCl molecules were obtained: 1.4×10^{-10} [133], 7.7×10^{-10} [134], 1.7×10^{-9} [49], 6.3×10^{-10} [57], 6.3×10^{-10} [10], 2.25×10^{-9} [82], 7.3×10^{-10} [60], and 8×10^{-10} cm^3 s^{-1} [107]. The rate constant K_{F_2} of KrF quenching by F_2 molecules took the following values: 7.8×10^{-10} cm^3 s^{-1} [135] (this constant is used in excimer laser simulation models [136–141, 22, 53, 10]), $(5.7 \pm 0.5) \times 10^{-10}$ [142], $(4.8 \pm 0.3) \times 10^{-10}$ [143], $(2.8 \pm 0.2) \times 10^{-10}$ [61], and $(3.0 \pm 0.3) \times 10^{-10}$ cm^3 s^{-1} [62].

In order to account for the uncertainty of the kinetic parameters, two groups of factors should be considered. They may be arbitrarily referred to as technical and physical. The former appears to be responsible for the difficulty of determining the exact composition of a gas mixture during K_{Q} measurements, due to the high chemical activity of halogens, especially that of F_2. Moreover, RgX^* relaxation kinetics can be markedly affected by quenching impurities such as CO_2, O_2, CO, NO, N_2O and halogenated compounds [60, 62].

The fact that neither K_{Q} nor τ_{re} is a constant provides the physical basis for the different K_{Q} measured. Indeed, the parameters of Eqn (54), K_{Q} and τ_{re}, depend on the molecular distribution over vibrational energy. A rise in the rate constants of quenching the electronic state D′ of halogen and interhalogen molecules by rare gas atoms while decreasing the store of vibrational energy in this state was first reported in Refs [144–147].

Let $K_{\mathrm{Q}}(\varepsilon)$ or $\tau_{\mathrm{re}}(\varepsilon)$ be approximated by the function $\varphi = a_0 + a_1\varepsilon + a_2\varepsilon^2$. Then for the vibrational distribution found from the Fokker–Planck equation (7) with parameters (8), $\tau_{\mathrm{u}} = \mathrm{const}$, $\rho = \mathrm{const}$, and (37), the mean φ can be written as [72]

$$\langle\varphi\rangle = (1+\varkappa)^{-2}\left[\varphi(0) + \varkappa(2+\varkappa)\varphi\left(\frac{1+\varkappa}{2+\varkappa}\,\varepsilon^*\right)\right]. \quad (55)$$

In other words, if k_{Q} and A_{i-l} are functions of ε, then the kinetic parameters K_{Q} and τ_{re} will depend on ε^* and the partial gas pressures (via $\varkappa$). Moreover, in a study of nonstationary processes, K_{Q} may vary with time because

$$K_{\mathrm{Q}} \equiv \frac{\int k_{\mathrm{Q}}(\varepsilon) f(\varepsilon, t)\,\mathrm{d}\varepsilon}{\int f(\varepsilon, t)\,\mathrm{d}\varepsilon}$$

by definition.

The dependence of a quantity being measured on the molecular distribution over vibrational energy was evaluated in Ref. [72]. The study was designed to analyze the intensity ratio $I_{\mathrm{b}}/I_{\mathrm{n}}$ of the broad (C → A, B → A′) band to narrow (B → X) band XeCl luminescence. In so doing the authors managed to make the analysis using no adjustable parameters. It is worthwhile examining the $I_{\mathrm{b}}/I_{\mathrm{n}}$ variation in more detail bearing in mind the importance of the problem in question and the discovery of certain surprising properties.

The following radiative transitions are known to be allowed for a XeCl excimer: B → X, C → A, and B → A′. The Einstein coefficients A_{i-l} of these transitions depend on ε [23–25]. In order to determine the functions $A_{i-l}(\varepsilon)$, one may take advantage of the results of *ab initio* calculations done on an all-electron configuration interaction in an RgX molecule with regard to the spin-orbit interaction in a semiempirical way [119]. The following parameters were calculated in Ref. [72] proceeding from the data reported in Ref. [119]: the Einstein coefficient $A(\varepsilon) = \int a(v, \varepsilon)\,\mathrm{d}v$; the mean transition wavelength $\lambda(\varepsilon) = cA / \int va\,\mathrm{d}v$; the linewidth of the bound-

free electronic-vibration transition

$$\Delta\lambda = \lambda\left[\frac{\int(\lambda v/c)^2 a\,\mathrm{d}v}{A} - 1\right]^{1/2};$$

here $a(v,\varepsilon)$ is the probability of spontaneous light emission with frequency v by a XeCl(B, C) molecule having vibrational energy ε, and c is the speed of light in vacuum. The data obtained are presented in Fig. 10.

The calculated transition wavelengths λ are shorter than the observed ones. For example, the emission B $\rightarrow$ X for the transition from the ground vibrational level possesses a wavelength of 308 nm, while the calculated $\lambda(0)$ value is 295 nm. Nevertheless, the radiative lifetime for XeCl(B, $v = 0 \rightarrow$ X) and XeCl(C, $v = 0 \rightarrow$ A) transitions, $\tau_B = 11.1 \pm 0.2$ and $\tau_C = 131 \pm 10$ ns [57], are in good agreement with the calculated values of $\tau_B \equiv 1/A_{B-X}(0) = 11$ and $\tau_C \equiv 1/A_{C-A}(0) = 120$ ns, respectively. It follows from Fig. 10a and formula (55) that

$$\langle A_{B-X}\rangle \simeq (1+\varkappa)^{-2}\tau_B^{-1}, \quad \langle A_{C-A}\rangle \simeq (1+\varkappa)^{-2}\tau_C^{-1},$$
$$\langle A_{B-A'}\rangle = (1+\varkappa)^{-2}\left[A_{B-A'}(0) + \varkappa(2+\varkappa)A_{B-A'}\left(\varepsilon^*\frac{1+\varkappa}{2+\varkappa}\right)\right], \tag{56}$$

where $\varepsilon^* \geqslant 1$ eV.

It can be seen from Figs 10b and 10c that the narrow-band emission by XeCl corresponds to the B $\rightarrow$ X transition. The intensity of this transition is

$$I_n = \frac{1}{2}\langle A_{B-X}\rangle N \equiv \frac{1}{\tau_{B-X}} N. \tag{57}$$

According to Refs [148, 149] and Fig. 10, the emission bands C $\rightarrow$ A and B $\rightarrow$ A$'$ overlap in such a way that they cannot be separated. Therefore, the intensity of broad-band emission is $I_b = (1/2)\big(\langle A_{C-A}\rangle + \langle A_{B-A'}\rangle\big)N$. Division of I_b by I_n yields the ratio $\vartheta \equiv I_b/I_n$, which is

$$\vartheta = \vartheta_0 + \varkappa(1+\varkappa)\tau_B A_{B-A'}\left(\varepsilon^*\frac{1+\varkappa}{2+\varkappa}\right), \tag{58}$$

where $\vartheta_0 \equiv \tau_B/\tau_C + \tau_B A_{B-A'}(0)$. The least possible value of ϑ calculated for a XeCl excimer is $\vartheta_0 = 0.15$.

Let us compare (58) and ϑ found on the assumption of equilibrium populations of XeCl(B) and XeCl(C) vibrational levels [148–150]:

$$\vartheta = \frac{k_C + \tau_B k_{BC}^Q (k_C + k_B)[Q]}{k_B + \tau_C k_{CB}^Q (k_C + k_B)[Q]}. \tag{59}$$

It is implied here that the buffer gas pressure $p > 70$ mbar. Parameters k_B and k_C were called RgX(B) and RgX(C) generation rates and k_{BC}^Q and k_{CB}^Q rate constants of collisional mixing between B and C states.

Formula (58) describes the nonmonotone dependence of ϑ on the buffer gas pressure p. At low p, the parameter $\varkappa$ is approximately equal to $(\tau_r/k_{VT}^Q)(1/[Q])$; hence, $\vartheta(1/p)$ is a linearly decreasing function of $1/p$. The minimum of ϑ occurs at a buffer gas concentration Q close to

$$[Q]_{min} \simeq \left(k_Q^Q \tau_r\right)^{-1/2}. \tag{60}$$

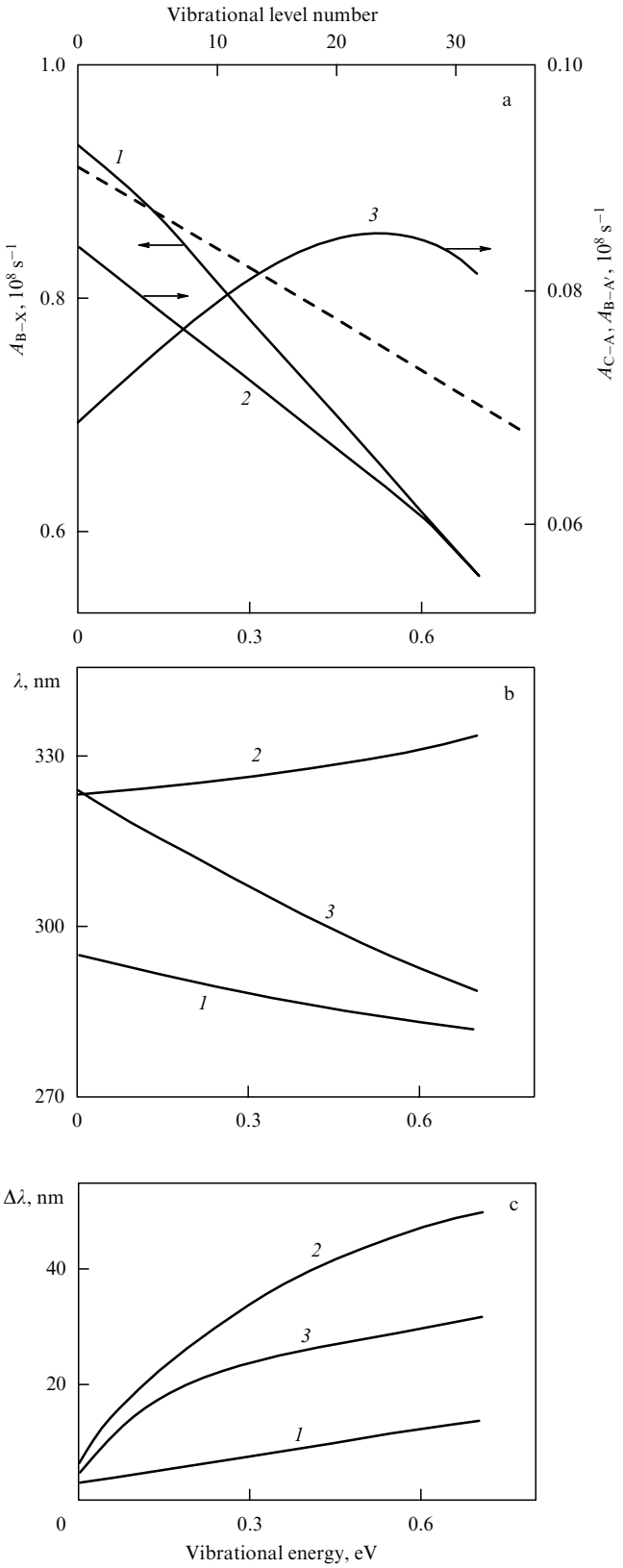

Figure 10. Parameters of transitions B $\rightarrow$ X (curve *1*), C $\rightarrow$ A (curve *2*), and B $\rightarrow$ A$'$ (curve *3*) in XeCl. The dashed line shows the $A_{B-X}(\varepsilon)$ dependence from Ref. [25].

At high buffer gas pressures, the parameter $\varkappa(p)$ grows as

$$\varkappa \simeq \frac{k_Q(0)}{k_{VT}} + \frac{k_Q^Q(0)}{k_{VT}}[Q].$$

Therefore, the $\vartheta(p)$ ratio must smoothly increase with increasing p.

Formula (59) describes the monotonic p-dependence of ϑ. The ϑ ratio varies from $\vartheta_l \simeq k_C/k_B$ at low p to $\vartheta_h \simeq (\tau_B/\tau_C)(k_{BC}^Q/k_{CB}^Q)$ in the limit of infinitely high pressures.

The nonmonotone p-dependence of ϑ predicted by formula (58) agrees fairly well with a number of experimental findings. Figure 11 taken from Ref. [150] shows the ϑ ratio measured over a broad range of Ar, He, and Ne pressures. For all buffer gases $\vartheta \geqslant 0.15$ in accordance with the ϑ_0 value found from (58).

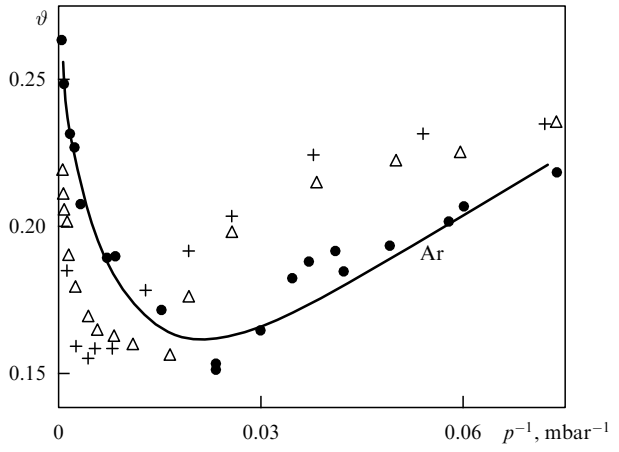

Figure 11. Intensity ratio ϑ for XeCl(B, C) luminescence as a function of argon (●), neon (+), and helium (△) inverse pressure.

The quantitative validation of Eqn (58) was carried out by computing the $\vartheta(\varepsilon^*, \varkappa)$ value, which corresponds to that obtained in an experiment in which ε^* and $\varkappa$ were fixed and ϑ was measured. In Ref. [59], XeCl(B) molecules with $\varepsilon^* = 1.2$ eV were generated in the process of two-photon absorption of laser radiation in a mixture of Cl_2 (2 mbar) and Xe (136 mbar). The vibrational temperature $T_v = 500$ K was determined from the shape of the time-integrated XeCl(B, $v = 0-3$) emission spectrum. According to Eqn (11), this T_v value corresponds to $\varkappa = 0.4$. Substitution of ε^* and $\varkappa$ into (58) gives $\vartheta = 0.24$ [72], in conformity with the measured value of $\vartheta = 0.29 \pm 0.05$.

Comparing theoretical and experimental ϑ values in the above example suggests that the calculated result [72] shown in Fig. 10a underestimates $A_{B-A'}(\varepsilon)$ at $\varepsilon > 0.6$ eV on evidence derived from Ref. [119]. In this case, there must be a considerable variation of ϑ values measured under different conditions. In the active media of electron-beam and electric discharge lasers, high-energy ($\varepsilon^* \approx D$) excimers are largely produced. Therefore, the parameter ϑ must have a higher value in these media. Moreover, the $\vartheta(p)$ function must grow smoothly at high p. When XeCl with low energy ϑ^* are formed, the ϑ value must be close to ϑ_0 and show a weak dependence on p.

This inference is in excellent agreement with experimental data. In the case of an electric discharge XeCl laser [151], a rise in the Ne pressure from 0 to 8 bar led to an increase of ϑ from 0.25 to 0.35. At an Ne pressure of between 10 and 15 bar, ϑ depended on the Xe pressure and varied over the range 0.32–0.38. In another study [149], XeCl molecules appeared to have low energy ε^*. The value of ϑ fell in the range 0.17 to 0.20 under changes of the buffer gas (Ar) pressure from 0.13 to 1 bar.

Evidently, $\vartheta(p)$ measurements can be used to estimate kinetic parameters. For example, it follows from the position of $[He]_{min}$ and $[Ne]_{min}$ minima in Fig. 11 and Eqn (60) that

$$k_{He}^{He} > k_{Ne}^{Ne}. \tag{61}$$

This inequality is at variance with the expected ratio of quenching rate constants for RgX. In an excimer laser model [99], for instance, the measured value $k_{Ne}^{Ne} = 1 \times 10^{-33}$ cm^6 s^{-1} [133] was used and the estimate was submitted for $k_{He}^{He} = 5 \times 10^{-34}$ cm^6 s^{-1}. However, other authors [152] reported a value of $k_{He}^{He} = 5 \times 10^{-32}$ cm^6 s^{-1} [153], which is two orders of magnitude higher and conforms to (61).

The above analysis has demonstrated that the broad-band to narrow-band luminescence intensity ratio ϑ can be found with the aid of a diffusion model of vibrational relaxation. In this model, ϑ depends on the energy ε^* of generated molecules and the buffer gas pressure p. There must be a similar dependence for the effective radiative lifetime τ_{re} and quenching rate constants K_Q. It is worthwhile emphasizing some interesting variations of τ_{re} and K_Q inherent to rare-gas halide excimers.

10.3 Effective radiative lifetimes

The parameter τ_{re} arises when the electronic relaxation equation (54) is derived. Evidently, for rare gas halides, it is defined as

$$\tau_{re}^{-1} = \frac{1}{2}\left(\langle A_{B-X}\rangle + \langle A_{C-A}\rangle + \langle A_{B-A'}\rangle\right). \tag{62}$$

The last formula can be rewritten as

$$\tau_{re}^{-1} = \frac{1}{2}\langle A_{B-X}\rangle(1 + \vartheta). \tag{63}$$

The right-hand side of (63) contains the parameter $\vartheta(\varepsilon^*, \varkappa)$. In order to find $\langle A_{B-X}\rangle(\varepsilon^*, \varkappa)$ in an actual case of KrF, XeCl relaxation at $\varepsilon^* \simeq D$, it is possible to use the first expression of system (56). Thus, both terms in the right-hand side of Eqn (63), and hence τ_{re}, depend on ε^* and $\varkappa$.

The following definition was generally accepted in modelling physical-chemical kinetics in the active media of excimer lasers [62, 59, 22, 61, 53, 148, 150, 154]:

$$\tau_{re}^{-1} = \frac{\tau_B^{-1} + K_{eq}\tau_C^{-1}}{1 + K_{eq}}, \tag{64}$$

where $K_{eq} = \exp\left[(T_{eB} - T_{eC})/T\right]$, $T_{eB} - T_{eC}$ is the energy separation between states B and C, and τ_B^{-1} and τ_C^{-1} are the Einstein coefficients for the spontaneous transitions B, $v = 0 \to X$, and C, $v = 0 \to A$, respectively. This expression for τ_{re} is based on the hypothesis of an equilibrium population of RgX(B) and RgX(C) vibrational levels, which allows for the transition $B \to A'$ in (64) to be neglected, since $A_{B-A'}(0) \ll A_{C-A}(0)$.

Formula (64) contains the parameter $T_{eB} - T_{eC}$ in the right-hand side. This being so, it should be possible to find its value from a kinetic study of RgX electron relaxation. Certainly, it would be wrong to use (64) and similar formulae for the intensity ratio of broad- to narrow-band RgX luminescence at $\varepsilon^* \gg T$. This accounts for the difference of the $T_{eB} - T_{eC}$ values reported in the scientific literature and

found in RgX(B, C) kinetic studies from those measured by precise spectroscopic methods. For example, a spectroscopic evaluation yielded $T_{eB} - T_{eC} = 90 \pm 2$ cm^{-1} for a XeCl molecule [155], whereas kinetic studies gave the following values: -5.4 ± 25 [156], 128 ± 35 [149], 180 [157, 158], 220 ± 40 [150, 148], 85 [57], -22 [159] and 280 cm^{-1} [151].

10.4 Quenching rate constants

A few problems are encountered in the determination of the quenching rate constants K_Q. To begin with, let us suppose that it is possible to neglect the dependence of quantities being measured on the shape of the function $f(\varepsilon, t)$, when the buffer gas pressure varies over a relatively broad range. In this case, the intensity of RgX(B $\to$ C) luminescence (57) must be related to the molecular concentration [Q] by the Stern–Volmer relationship [160, 161]:

$$\frac{R}{I_n} = 1 + \vartheta + \tau_{B-X} \sum_Q \left(K_Q + \sum_M K_Q^M [M] \right) [Q] N . \qquad (65)$$

Here, R, ϑ, τ_{B-X}, K_Q, and K_Q^M are supposed to be independent of [Q]. Item ϑ in the right-hand side of (65) takes into account RgX(C $\to$ A) and RgX(B $\to$ A′) emissions.

It should be appropriate to characterize the quenching of XeCl(B) luminescence in an atmosphere of Ne by the rate constant $K_{Ne} = (0.76 \pm 0.15) \times 10^{-12}$ cm^3 s^{-1} measured from the decay of XeCl(B $\to$ X) luminescence [59].

From the relaxation equation (54), it is easy to find an expression similar in form to equality (65) using no simplified propositions:

$$\frac{R}{I_n} = 1 + \vartheta(f) + \tau_{B-X}(f) \sum_Q \left(K_Q(f) + \sum_M K_Q^M(f) [M] \right) [Q] N . \qquad (66)$$

The last expression takes into account that the parameters of Eqn (54) depend on the behaviour of the distribution function $f(\varepsilon, t)$ with respect to vibrational energy. In principle, the parameters ϑ, τ_{B-X}, K_Q, K_Q^M of the generalized Stern–Volmer equation (66) may depend on [Q]. Indeed, the data shown in Fig. 11 at [Ne] $\ll 3.3 \times 10^{19}$ cm^{-3} can be presented in the form [72]

$$\vartheta = \vartheta_l + \tau_{B-X} K_{Ne}^* [Ne] , \qquad (67)$$

where $K_{Ne}^* = (0.8 \pm 0.4) \times 10^{-12}$ cm^3 s^{-1}. Substituting (67) into (66) and comparing terms linear in [Ne] with the corresponding items in the dependence $R/I_n([Ne])$ (65), we arrive at

$$(0.8 \pm 0.4) \times 10^{-12} \text{ cm}^3 \text{ s}^{-1} + K_{Ne} = (0.76 \pm 0.15) \times 10^{-12} \text{ cm}^3 \text{ s}^{-1} .$$

Hence, the excimer deexcitation rate constant $\langle k_{Ne} \rangle = K_{Ne}$ may be disregarded in comparison with the measured quenching rate constant for XeCl(B $\to$ X) luminescence, $K_{Ne} = 0.76 \times 10^{-12}$ cm^3 s^{-1}. It should be noted that we compare the parameter $\langle k_Q \rangle$ in the relaxation equation (54) with the parameter K_Q of the Stern–Volmer equation (65). In the scientific literature, excimer deexcitation rate constants are usually referred to as quenching rate constants so as to emphasize that the parameter $\langle k_Q \rangle$ of molecular kinetics does not in any way differ from the K_Q constant which characterizes the quenching of luminescence.

This example shows that the use of this commonly accepted terminology may be regarded as an implicit assumption which does not have to be fulfilled. Therefore, considering the dependence of kinetic parameters on the form of function $f(\varepsilon, t)$ is important for understanding the physical nature of the phenomena observed.

Let us examine here the distinction between two widely applied techniques for the measurement of $K_Q \equiv \langle k_Q \rangle$. Measuring K_Q by the Stern–Volmer approach yields time-averaged quantities. In this case, the distribution function possesses the properties described in Section 3. When $k_Q(\varepsilon)$ is a sufficiently smooth function, $\langle k_Q \rangle$ can be estimated from expression (55). In the general case, for $k_Q(\varepsilon) = \sum_n a_n \varepsilon^n$ it is found that

$$\langle k_Q \rangle = \sum_n a_n \langle \varepsilon^n \rangle . \qquad (68)$$

Here, $\langle \varepsilon^n \rangle$ is a quantity of order $\varkappa(\varepsilon^*)^n$. Thus, the result of K_Q measurement by the Stern–Volmer method is essentially dependent on the energy ε^* of the molecules created and the gas mixture composition ($\varkappa$).

Another common approach to the evaluation of K_Q is based on the measurement of the pulse luminescence decay time as a function of [Q]. It was shown in Section 8 that at the instant the measurement is taken the function $f(\varepsilon, t)$ is close to the equilibrium distribution function (39) with $T_v = T$ and $N = N_0 \exp(-t/\tau_u)$. For such a distribution, the moments $\langle \varepsilon^n \rangle$ constitute quantities of order T^n [see Eqn (40)]. Therefore, it follows from (68) that

$$K_Q \equiv \langle k_Q \rangle = k_Q(0) . \qquad (69)$$

Hence, the result of the measurement of K_Q is related to neither ε^* nor $\varkappa$, and the luminescence quenching rate constant K_Q thus found will be identical to the rate constant $k_Q(0)$ of low vibrational level deexcitation in excimers.

Let us compare the rate constants K_Q measured by the above two methods. When the excimers created during measurements using the Stern–Volmer method have low ε, both the techniques produce a similar result (69). Let the energy of the molecules being formed be $\varepsilon^* \approx D$. In this case, the results of measurements according to (66) will depend on the shape of the function $k_Q(\varepsilon)$. Let us further analyze this dependence on the assumption that $k_Q(\varepsilon)$ is either a decreasing, constant or increasing function of ε. For simplicity, we shall suppose that the first equality in (56) can be used in calculating $\langle A_{B-X}(\varepsilon) \rangle$.

Let $k_Q(\varepsilon)$ be a decreasing function of ε similar to the function $A_{B-X}(\varepsilon)$. Then $k_Q(\varepsilon)$ is smaller than (69), viz.

$$\langle k_Q \rangle \simeq \frac{1}{(1+\varkappa)^2} k_Q(0) . \qquad (70)$$

The factor $(1+\varkappa)^{-2}$ for active media of excimer lasers normally varies between 0.5 and 0.7. Interestingly, Eqn (66) includes the product

$$\tau_{B-X}(\varkappa) K_Q(\varkappa) = 2 \frac{k_Q(0)}{A_{B-X}(0)} ,$$

which is independent of both ε^* and $\varkappa$.

Let us assume k_Q to be independent of ε. In this case, the luminescence quenching rate constant K_Q will be certainly defined by the equality (69). However, the value of $\tau_{B-X} K_Q$

measured by the Stern – Volmer method will depend on the gas mixture composition:

$$\tau_{B-X}(\varkappa)K_Q = 2(1+\varkappa)^2\frac{k_Q(0)}{A_{B-X}(0)}\,.$$

The variation of K_Q will be especially well apparent when $k_Q(\varepsilon)$ is an increasing function of ε. The higher ε^* the larger K_Q as compared with (69). Evidently, the constants K_Q found according to (66) and from nonstationary luminescence decay will be different. This inference can be illustrated by the following examples.

In a series of experiments (see Table 10) [143, 163, 162], the vibrationally excited KrF(B, C) molecules were generated by photodissociation of KrF_2 molecules:

$$KrF_2 + \frac{hc}{\lambda_p} \rightarrow KrF^* + F\,. \qquad (71)$$

Photolysis of KrF_2 vapors using a broad-band radiation with $\lambda_p = 110-180$ nm [162] resulted in the appearance of a structureless absorption band with a maximum at 162 nm and a half-width of 21 nm. Measurements taken in a pure KrF_2 vapor ($p < 1$ mbar) yielded a $K_{KrF_2}\tau_{re}$ product of $(19.7 \pm 1.4) \times 10^{-18}$ cm^3. After a buffer gas (N_2) with $p = 66$ mbar was added to the KrF_2, the vibrational excitation of KrF^* decreased and the $K_{KrF_2}\tau_{re}$ value was decreased two-fold to $(10.2 \pm 1.4) \times 10^{-18}$ cm^3 (see Table 10).

Table 10. Changes of $K_{KrF_2}\tau_{re}$ for the KrF(B, C) excimer.

p, mbar	Mixture	$K_{KrF_2}\tau_{re}$, 10^{-18} cm^3	Ref.
< 1	KrF_2	19.7 ± 1.4	[162]
66	$KrF_2 - N_2$	10.2 ± 1.4	
0.26 – 1.7	KrF_2	0.95	[143]
2000	$KrF_2 - CF_4 - N_2 - He$	0.42	[163]
	$KrF_2 - CF_4 - Kr - He$		
	$KrF_2 - CF_4 - N_2 - Kr - He$		

Excitation of pure KrF_2 vapors by ArF(B – X) radiation with $\lambda_p = 193$ nm resulted in a one order of magnitude smaller value of $K_{KrF_2}\tau_{re} = 9.5 \times 10^{-19}$ cm^3, so that $K_{KrF_2} = 1.4 \times 10^{-10}$ cm^3 s^{-1} [143]. A salient difference between the two experiments [162] and [143] consisted in pumping with different λ_p. It is clear that the KrF^* molecules generated by the process (71) at $\lambda_p \simeq 162$ nm must have an energy ε^* approximately 1.3 eV higher than in the case of KrF_2 photolysis by radiation with $\lambda_p = 193$ nm. Therefore, the discrepancy between the measurements of $K_{KrF_2}\tau_{re} = \langle k_{KrF_2}\rangle\tau_{re}$ should be attributed to a rise in $k_{KrF_2}(\varepsilon)$ with increasing ε. If this explanation is correct, then the measurement of $K_{KrF_2}\tau_{re}$ at $\lambda_p \simeq 162$ nm and buffer gas pressure of a few bars should lead to $K_{KrF_2}\tau_{re} \ll 10^{-17}$ cm^3 s^{-1}. Such an experiment has just been reported in Ref. [163].

The study [163] was organized as a series of three experiments on the excitation of KrF_2-based mixtures by broad-band radiation from an open high-current discharge. The luminance temperature of the pumping source in the spectral region 150 – 180 nm amounted to 35 kK. The first experiment was designed to excite a mixture of KrF_2 (2.2 mbar) – CF_4 (0.33 bar) – N_2 (0.4 bar) – He (1.26 bar). In the second one, a mixture of KrF_2 (2.2 mbar) – CF_4 (0.33 bar) – Kr (0.15 bar) – He (1.51 bar) was excited, and the third experiment was concerned with the excitation of a KrF_2 (2.2 mbar) – CF_4 (0.33 bar) – N_2 (0.4 bar) – Kr (0.15 bar) – He (1.11 bar) mixture. By comparing the Kr_2F^* luminescence intensities in the three experiments, the rate constant $K_{KrF_2} = 6.2 \times 10^{-10}$ cm^3 s^{-1} corresponding to $K_{KrF_2}\tau_{re} = 4.2 \times 10^{-19}$ cm^3 was found.

It can be seen from above findings that the introduction of a diluting gas with $p = 2$ bars into the test mixtures invariably resulted in an almost 50-fold decrease of $K_{KrF_2}\tau_{re}$ despite a similar mechanism of KrF^* formation.

Active media of excimer lasers are normally excited by an electron beam or electric discharge. Such pumping produces excimer species with $\varepsilon^* = D$ largely by ionic recombination. For XeCl and KrF molecules, D is 4.2 and 5.3 eV, respectively. In excimer laser models, the following rate constants are used: $K_{HCl} = 1.7 \times 10^{-9}$ cm^3 s^{-1} for XeCl luminescence quenching by HCl molecules [99, 49], and $K_{F_2} = 0.8 \times 10^{-9}$ cm^3 s^{-1} for KrF luminescence quenching by F_2 [135, 22, 53, 139, 141, 140]. These rate constants are several times higher than the characteristics of decaying luminescence (69) in so far as $K_{HCl} = 7.3 \times 10^{-10}$ cm^3 s^{-1} for XeCl [60] and $K_{F_2} = 3 \times 10^{-10}$ cm^3 s^{-1} for KrF [61].

To summarize, the theory of vibrational relaxation suggests one possible cause for the extremely broad variability of results of different measurements of one and the same kinetic parameter K_Q. In both experimental studies and excimer electronic relaxation modelling, it is necessary to take into consideration the dependences of K_Q and τ_{re} on the mean vibrational energy $\langle\varepsilon\rangle$. In turn, the value of $\langle\varepsilon\rangle$ shows a dependence on the inner energy ε^* of the molecules produced and the parameter $\varkappa$, i.e. on the gas mixture composition. Moreover, it should be borne in mind that the values of $K_Q = \langle k_Q(\varepsilon)\rangle$ and (63), which characterize time-averaged and quasi-stationary processes, may differ from the corresponding values of (69) and (64) measured from nonstationary luminescence decay [62, 59 – 61].

11. Conclusions

This review is concerned with the vibrational relaxation of electronically excited molecules. It presents a comparative analysis of different relaxation models along with experimentally obtained values for the vibrational relaxation rate constants used in these models. Through the progress made in modelling excimer electron-vibration kinetics such phenomena as the dependence of quantum yields of spontaneous and stimulated emission on the vibrational relaxation rate were understood as well as the luminescence kinetics of electronically excited molecules.

It should be emphasized that several questions related to the dynamics of electronic and vibration transitions were investigated rather poorly. Thus the scientific literature fails to include data permitting rigorous determination of vibrational-energy-dependence of relaxation rates. This particularly concerns the excimer collisional deexcitation rates.

Despite the marked difficulty in the theoretical examination of the problem, the following most essential features of vibrational distributions have been established rather reliably. To be exact, the low vibrational levels of excimers are most densely populated in the active media of lasers, with vibrational distributions close to the Boltzmann ones. In the region of high vibrational energy levels, however, the distribution has a plateau shape. It is crucial that the mean energy of real vibrational distributions is much higher than the thermal energy. In other words, a high proportion of

molecules populate a large number of upper vibrational levels.

To summarize, the results presented in this review make it possible to better understand specific features of molecular relaxation stemming from the nonequilibrium population of vibrational levels. On the other hand, the kinetic peculiarities studied may be of value in current and future investigations with the object of further improving the performance of excimer lasers.

The authors wish to thank A V Eletskiĭ for discussing the diffusion model of vibrational relaxation. We are also grateful to D W Setser, F P Schäfer, M J Shaw, S Szatmari, V S Zuev, I P Vinogradov, and A N Oraevskiĭ for general advice on many problems touched upon in this review.

References

1. Eletskiĭ A V *Usp. Fiz. Nauk* **125** 279 (1978) [*Sov. Phys. Usp.* **21** 502 (1978)]
2. Gudzenko L I, Yakovlenko S I *Plazmennye Lazery* (Plasma Lasers) (Moscow: Atomizdat, 1978)
3. Lakoba I S, Yakovlenko S I *Kvantovaya Elektron.* **7** 677 (1980) [*Sov. J. Quantum Electron.* **10** 389 (1980)]
4. Smirnov B M *Usp. Fiz. Nauk* **139** 53 (1983) [*Sov. Phys. Usp.* **26** 31 (1983)]
5. Eletskiĭ A V, Smirnov B M *Fizicheskie Protsessy v Gazovykh Lazerakh* (Physical Processes in Gaseous Lasers) (Moscow: Energoatomizdat, 1985)
6. Popov V K *Usp. Fiz. Nauk* **147** 587 (1985) [*Sov. Phys. Usp.* **28** 1031 (1985)]
7. McDaniel E, Nighan U (Eds) *Gas Lasers* (Applied Atomic Collision Physics, Vol. 3) (New York, London: Academic Press, 1982) [Translated into Russian (Moscow: Mir, 1986)]
8. Molchanov A G *Tr. Fiz. Inst. Akad. Nauk SSSR* **171** 54 (1986)
9. Baranov V Yu, Borisov V M, Stepanov Yu Yu *Élektrorazryadnye Éksimernye Lazery na Galogenidakh Inertnykh Gazov* (Electric Discharge Excimer Lasers in Inert Gas Halides) (Moscow: Energoatomizdat, 1988)
10. Boĭchenko A M et al. *Tr. IOFAN* **21** 44 (1989)
11. Lacour B, in *High Power Lasers — Science and Engineering* (Eds R Kossowsky, M Jelinek, R F Walter) (Dordrecht: Kluwer Academic Publishers, 1996)
12. Baĭko I Yu, Istomin E A, Poĭzner B N *Kvantovaya Elektron.* **21** 1103 (1994) [*Quantum Electron.* **24** 1025 (1994)]
13. Basov N G et al. *Kvantovaya Elektron.* **18** 902 (1991) [*Sov. J. Quantum Electron.* **21** 816 (1991)]
14. Szatmari S *Appl. Phys. B* **58** 211 (1994)
15. Angood S et al. *Specification for the TITANIA* KrF *Laser System* RAL-94-014 (Rutherford Appleton Laboratory: Science and Engineering Research Council, 1994)
16. Owadano Y et al. *The Fourth International Workshop on* KrF *Laser Technology* (Annapolis, MD, 1994)
17. *Nike* KrF *Laser Facility* NRL/PU/6430–95-289 (Washington: Naval Research Laboratory, 1995)
18. Joshi C J, Corkum P B *Physics Today* **48** 36 (1995)
19. Jacob J H et al. *J. Appl. Phys.* **50** 5130 (1979)
20. Pummer H, Hohla K, Rebentrost F *Appl. Phys.* **20** 129 (1979)
21. Jacob J H et al. *Appl. Phys. Lett.* **37** 522 (1980)
22. Kannari F, Obara M, Fujioka T *J. Appl. Phys.* **57** 4309 (1985)
23. Dreiling T D, Setser D W *J. Chem. Phys.* **75** 4360 (1981)
24. Morgan W L, Winter N W, Kulander K C *J. Appl. Phys.* **54** 4275 (1983)
25. Kvaran A, Shaw M J, Simons J P *Appl. Phys. B* **46** 95 (1988)
26. Corkum P B, Taylor R S *IEEE J. Quantum Electron.* **QE-18** 1962 (1982)
27. Szatmari S, Schäfer F P *J. Opt. Soc. Am. B* **4** 1943 (1987)
28. Bourne O L, Alcock A J *Appl. Phys. B* **32** 193 (1983)
29. Losev S A, Generalov N A *Dokl. Akad. Nauk SSSR* **141** 1072 (1961) [*Sov. Phys. Dokl.* **6** 1081 (1962)]
30. Stupochenko E V, Losev S A, Osipov A I *Relaksatsionnye Protsessy v Udarnykh Volnakh* (Relaxation in Shock Waves) (Moscow: Nauka, 1965) [Translated into English (New York: Springer-Verlag, 1967)]
31. Zel'dovich Ya B, Raĭzer Yu P *Fizika Udarnykh Voln i Vysokotemperaturnykh Gidrodinamicheskikh Yavleniĭ* (Physics of Shock Waves and High-Temperature Hydrodynamic Phenomena) (Moscow: Nauka, 1966) [Translated into English (New York: Academic Press, 1966 – 1967)]
32. Losev S A, Shatalov O P, Yalovik M S *Dokl. Akad. Nauk SSSR* **195** 585 (1970) [*Sov. Phys. Dokl.* **15** 1037 (1971)]
33. Gordiets B F, Markov M N, Shelepin L A *Kosmich. Issled.* **8** 437 (1970) [*Cosmic Res.* **8** 398 (1970)]
34. Basov N G et al. *Dokl. Akad. Nauk SSSR* **198** 1043 (1971)
35. Smirnov B M *Fizika Slaboionizovannogo Gaza* (Physics of Weakly Ionized Gases) (Moscow: Nauka, 1972) [Translated into English (Moscow: Mir Publishers, 1981)]
36. Safaryan M N *Zh. Prikl. Mekh. Tekh. Fiz.* (2) 38 (1974)
37. Oraevskiĭ A N, Stepanov A A, Shcheglov V A *Kvantovaya Elektron.* **1** 1166 (1974) [*Sov. J. Quantum Electron.* **4** 638 (1974)]
38. Likal'ter A A *Zh. Prikl. Mekh. Tekh. Fiz.* (3) 8 (1975)
39. Safaryan M N, Skrebkov O V *Fiz. Goreniya Vzryva* **11** 614 (1975)
40. Belenov É M et al. *Kvantovaya Elektron.* **2** 1629 (1975) [*Sov. J. Quantum Electron.* **5** 880 (1975)]
41. Gordiets B F, Mamedov Sh S *Kvantovaya Elektron.* **2** 1992 (1975) [*Sov. J. Quantum Electron.* **5** 1082 (1975)]
42. Losev S A *Gazodinamicheskie Lazery* (Gasodynamic Lasers) (Moscow: Nauka, 1977) [Translated into English (Berlin, New York: Springer-Verlag, 1981)]
43. Nikitin E E, Osipov A I *Kolebatel'naya Relaksatsiya v Gazakh* (Vibrational Relaxation in Gases) (Moscow: VINITI Publ., 1977)
44. Gordiets B F, Osipov A I, Shelepin L A *Kineticheskie Protsessy v Gazakh i Molekulyarnye Lazery* (Kinetic Processes in Gases and Molecular Lasers) (Moscow: Nauka, 1980) [Translated into English (New York: Gordon and Breach Science Publishers, 1988)]
45. Shelepin L A, in *Principles of Laser Plasma* (Ed. G Bekefi) (New York: John Wiley & Sons, 1976) [Translated into Russian (Moscow: Energoizdat, 1982) p. 8]
46. Reshetnyak S A, Shelepin L A *Tr. Fiz. Inst. Akad. Nauk SSSR* **144** 37 (1984)
47. Sauer M C, Jr. et al. *J. Chem. Phys.* **64** 4587 (1976)
48. Koffend J B, Sibai A M, Bacis R *J. Phys.* (Paris) **43** 1639 (1982)
49. Tisone G C, Hoffman J M *IEEE J. Quantum Electron.* **QE-18** 1008 (1982)
50. Kannari F et al. *IEEE J. Quantum Electron.* **QE-19** 232 (1983)
51. Kannari F et al. *IEEE J. Quantum Electron.* **QE-19** 1587 (1983)
52. Mandl A *J. Appl. Phys.* **59** 1435 (1986)
53. Kannari F, Shaw M J, O'Neil F *J. Appl. Phys.* **61** 476 (1987)
54. Kannari F *J. Appl. Phys.* **67** 3954 (1990)
55. Badziak J *Acta Phys. Pol. A* **78** 697 (1990)
56. Sergeev P B *Kratk. Soobshch. Fiz.* (FIAN) (5) 7 (1988)
57. Inoue G, Ku J K, Setser D W *J. Chem. Phys.* **80** 6006 (1984)
58. Rubin R J, Shuler K E *J. Chem. Phys.* **25** 59, 68 (1956)
59. Quinones E et al. *J. Chem. Phys.* **93** 333 (1990)
60. Yu Y C, Wategaonkar S J, Setser D W *J. Chem. Phys.* **96** 8914 (1992)
61. Gadomski W et al. *Chem. Phys. Lett.* **189** 153 (1992)
62. Xu J, Gadomski W, Setser D W *J. Chem. Phys.* **99** 2591 (1993)
63. Datsyuk V V, Izmaĭlov I A, Kochelap V A *Kvantovaya Elektron.* **13** 2120 (1986) [*Sov. J. Quantum Electron.* **16** 1398 (1986)]
64. Datsyuk V V, Izmaĭlov I A, Kochelap V A *Opt. Spektrosk.* **61** 1013 (1986)
65. Datsyuk V V, Izmaĭlov I A, Kochelap V A *Khim. Fiz.* **6** 304 (1987)
66. Datsyuk V V, Izmaĭlov I A, Kochelap V A *Kvantovaya Elektron.* **15** 106 (1988) [*Sov. J. Quantum Electron.* **18** 67 (1988)]
67. Datsyuk V V, Izmaĭlov I A, Kochelap V A *Opt. Spektrosk.* **69** 802 (1990)
68. Datsyuk V V, Izmaĭlov I A, Kochelap V A *Appl. Phys. B* **52** 22 (1991)
69. Datsyuk V V *Appl. Phys. B* **55** 60 (1992)
70. Datsyuk V V, Izmaĭlov I A *Kvantovaya Elektron.* **20** 129, 316 (1993)
71. Datsyuk V V, Izmaĭlov I A, Kochelap V A *Ukr. Fiz. Zh.* **38** 242 (1993)
72. Datsyuk V V *J. Chem. Phys.* **102** 799 (1995)
73. Adamovich V A et al. *Kvantovaya Elektron.* **14** 80 (1987) [*Sov. J. Quantum Electron.* **17** 45 (1987)]

74. Lo G, Setser D W *J. Chem. Phys.* **100** 5432 (1994)
75. Gorban' I S et al. *Kvantovaya Elektron.* (Kiev) **30** 38 (1986)
76. Zubrilin N G, Chernomorets M P *Kvantovaya Elektron.* **18** 170 (1991) [*Sov. J. Quantum Electron.* **21** 150 (1991)]
77. Schatzlein E et al. *Appl. Phys. B* **27** 49 (1982)
78. Nai-Ho Cheung, Cool T A, Erlandson A C *J. Chem. Phys.* **86** 6203 (1987)
79. Kvaran A, Sigurdardottir I D, Simons J P *J. Phys. Chem.* **88** 6383 (1984)
80. Danilychev V A et al. *Kvantovaya Elektron.* **14** 399 (1987)
81. Suda A, Obara M, Noguchi A *J. Appl. Phys.* **58** 1129 (1985)
82. Adamovich V A et al. *Kvantovaya Elektron.* **17** 1395 (1990) [*Sov. J. Quantum Electron.* **20** 1303 (1990)]
83. Grattan K T V, Hutchinson M H R, Thomas K J *Opt. Commun.* **39** 303 (1981)
84. Datsyuk V *The Fourth International Workshop on* KrF *Laser Technology* (Annapolis, MD, 1994)
85. Rokni M et al. *Appl. Phys. Lett.* **36** 243 (1980)
86. Zuev V S, Mikheev L D, Shirokikh A P *Kvantovaya Elektron.* **9** 573 (1982) [*Sov. J. Quantum Electron.* **12** 342 (1982)]
87. Baboshin V N et al. *Kvantovaya Elektron.* **8** 1138 (1981) [*Sov. J. Quantum Electron.* **11** 683 (1981)]
88. Abramowitz M, Stegun I (Eds) *Handbook of Mathematical Functions, with Formulas, Graphs, and Mathematical Tables* (New York: Dover Publications, 1965) [Translated into Russian (Moscow: Nauka, 1979)]
89. Shaw M J et al. *Appl. Phys. Lett.* **37** 346 (1980)
90. Fulghum S F, Feld M S, Javan A *IEEE J. Quantum Electron.* **QE-16** 815 (1980)
91. Hsia J C et al. *Appl. Phys. Lett.* **34** 208 (1979)
92. Tuxworth R W, Lawton M, Shaw M J *J. Phys. D* **13** 135 (1980)
93. Kimura W D, Moody S E, Seamans J F *Appl. Phys. Lett.* **49** 255 (1986)
94. Litzenberger L, Mandl A *Appl. Phys. Lett.* **52** 1557 (1988)
95. Hirst G J, Shaw M J *Appl. Phys. B* **52** 331 (1991)
96. Lee Y W et al. *Opt. Commun.* **94** 546 (1992)
97. Eletskiĭ A V, Smirnov B M *Zh. Eksp. Teor. Fiz.* **84** 1639 (1983) [*Sov. Phys. JETP* **57** 955 (1983)]
98. Trainor D W, Jacob J H *Appl. Phys. Lett.* **37** 675 (1980)
99. Hokazono H et al. *J. Appl. Phys.* **56** 680 (1984)
100. Smirnov B M *Atomnye Stolknoveniya i Élementarnye Protsessy v Plazme* (Atomic Collisions and Elementary Processes in Plasma) (Moscow: Atomizdat, 1968)
101. Smirnov B M *Iony i Vozbuzhdennye Atomy v Plazme* (Ions and Excited Atoms in Plasma) (Moscow: Atomizdat, 1974)
102. Hazi A U, Rescigno T N, Orel A E *Appl. Phys. Lett.* **35** 477 (1979)
103. Eletskiĭ A V, Smirnov B M *Zh. Tekh. Fiz.* **38** 3 (1968)
104. Smirnov B M *Otritsatel'nye Iony* (Negative Ions) (Moscow: Atomizdat, 1978) [Translated into English (New York, London: McGraw-Hill, 1982)]
105. Eletskiĭ A V, Smirnov B M *Usp. Fiz. Nauk* **147** 459 (1985) [*Sov. Phys. Usp.* **28** 956 (1985)]
106. Kushner M J, Hanson D E, Schneider B I *Appl. Phys. Lett.* **55** 2482 (1989)
107. Kaul' V B, Kunts S É, Mel'chenko S V *Kvantovaya Elektron.* **22** 555 (1995) [*Quantum Electron.* **25** 529 (1995)]
108. Borisov V M et al. *Kvantovaya Elektron.* **12** 1641 (1985) [*Sov. J. Quantum Electron.* **15** 1081 (1985)]
109. Dem'yanov A V et al. *Kvantovaya Elektron.* **13** 1250 (1986) [*Sov. J. Quantum Electron.* **16** 817 (1986)]
110. Blinov I O et al. *Kvantovaya Elektron.* **15** 2441 (1988) [*Sov. J. Quantum Electron.* **18** 1531 (1988)]
111. Dem'yanov A V et al. *Kvantovaya Elektron.* **19** 848 (1992)
112. Dem'yanov A V et al. *Kvantovaya Elektron.* **22** 673 (1995) [*Quantum Electron.* **25** 645 (1995)]
113. Longo S et al. *Appl. Phys. B* **54** 239 (1992)
114. Boĭchenko A M et al. *Kvantovaya Elektron.* **19** 486 (1992) [*Sov. J. Quantum Electron.* **22** 444 (1992)]
115. Eletskiĭ A V *Zh. Tekh. Fiz.* **56** 850 (1986) [*Sov. Phys. Tech. Phys.* **31** 517 (1986)]
116. Klementov A D, Morozov N V, Sergeev P B *Kvantovaya Elektron.* **12** 1607 (1985) [*Sov. J. Quantum Electron.* **15** 1060 (1985)]
117. Klementov A D, Morozov N V, Sergeev P B *Kvantovaya Elektron.* **13** 1730 (1986) [*Sov. J. Quantum Electron.* **16** 1139 (1986)]
118. Klementov A D, Morozov N V, Sergeev P B *Kvantovaya Elektron.* **15** 276 (1988) [*Sov. J. Quantum Electron.* **18** 174 (1988)]
119. Hay P J, Dunning T H, Jr. *J. Chem. Phys.* **69** 2209 (1978)
120. Alekhin A A et al. *Zh. Tekh. Fiz.* **63** (2) 43 (1993) [*Tech. Phys.* **38** 80 (1993)]
121. Alekhin A A et al. *Zh. Tekh. Fiz.* **63** (2) 65 (1993) [*Tech. Phys.* **38** 91 (1993)]
122. Datsyuk V V, Izmaĭlov I A *Kvantovaya Elektron.* (Kiev) **40** 25 (1991)
123. Dunning T H, Jr., Hay P J *J. Chem. Phys.* **69** 134 (1978)
124. Sze R C, in *Top. Meet. Excim. Lasers Dig. Techn. Pap.* (New York, 1979) p. Tu A 8/1
125. Pikaev A K *Khim. Vys. Energ.* **19** 196 (1985)
126. Datsyuk V V, Izmaĭlov I A, Kochelap V A *Pis'ma Zh. Tekh. Fiz.* **14** 432 (1988) [*Sov. Tech. Phys. Lett.* **14** 193 (1988)]
127. Blauer J A et al. *Appl. Opt.* **23** 4352 (1984)
128. Zhao Q, Szatmari S, Schäfer F P *Appl. Phys. B* **47** 325 (1988)
129. Taylor A J, Gibson R B, Roberts J P *Appl. Phys. Lett.* **52** 773 (1988)
130. Basov N G (Ed.) *Khimicheskie Lazery* (Chemical Lasers) (Moscow: Nauka, 1982) [Translated into English (Berlin, New York: Springer-Verlag, 1990)]
131. Gerber T, Lüthy W, Burkhard P *Opt. Commun.* **35** 242 (1980)
132. Kochelap V A, Datsyuk V V, Izmaĭlov I A *J. Phys. IV* **1** C7-583 (1991)
133. Finn T G et al. *Appl. Phys. Lett.* **36** 789 (1980)
134. Levin L A et al. *IEEE J. Quantum Electron.* **QE-17** 2282 (1981)
135. Rokni M, Jacob J H, Mangano J A *Phys. Rev. A* **16** 2216 (1977)
136. Rokni M et al. *IEEE J. Quantum Electron.* **QE-14** 464 (1978)
137. Greene A E, Brau C A *IEEE J. Quantum Electron.* **QE-14** 951 (1978)
138. Karasawa S, Shimauchi H *J. Specrosc. Soc. Jpn* **28** 308 (1979)
139. Morgan W L, Szöke A *Phys. Rev. A* **23** 1256 (1981)
140. Shaw M J *Appl. Phys. B* **30** 5 (1983)
141. Mandl A, Klimek D, Parks J H *J. Appl. Phys.* **55** 3940 (1984)
142. Quigley G P, Hughes W M *Appl. Phys. Lett.* **32** 627 (1978)
143. Eden J G et al. *Appl. Phys. Lett.* **32** 733 (1978)
144. Bibinov N K, Vinogradov I P, Mikheev L D *Kvantovaya Elektron.* **10** 833 (1983) [*Sov. J. Quantum Electron.* **13** 516 (1983)]
145. Bibinov N K et al. *Usp. Fotoniki* (8) 51 (1983)
146. Bibinov N K, Vinogradov I P *Khim. Fiz.* **7** 297, 455 (1988)
147. Vinogradov I P Thesis for Doctorate of Physicomathematical Sciences (Leningrad: A A Zhdanov Leningrad State University, 1990)
148. Yu Y C, Setser D W, Horiguchi H *J. Phys. Chem.* **87** 2199 (1983)
149. Tellinghuisen J, McKeever M R *Chem. Phys. Lett.* **72** 94 (1980)
150. Brashears H C, Jr., Setser D W *J. Phys. Chem.* **84** 224 (1980)
151. Lo D, Zheng C-E *J. Phys. D* **20** 714 (1987)
152. Braginskiĭ V M et al. *Kvantovaya Elektron.* **13** 751 (1986) [*Sov. J. Quantum Electron.* **16** 488 (1986)]
153. Misunami M et al. *Rev. Laser Eng.* **9** 512 (1981)
154. Lee Y-W, Endoh A *Appl. Phys. B* **52** 245 (1991)
155. Jouvet C, Lardeux-Dedonder C, Solgadi D *Chem. Phys. Lett.* **156** 569 (1989)
156. Bokor J, Rhodes C K *J. Chem. Phys.* **73** 2626 (1980)
157. Grieneisen H P, Hu Xue-Jing, Kompa K L *Chem. Phys. Lett.* **82** 421 (1981)
158. Marowsky G et al. *J. Chem. Phys.* **75** 1153 (1981)
159. Le Calvé J et al., in *Photophysics and Photochemistry Above* 6 *eV* (Ed. F Lahmani) (Amsterdam: Elsevier, 1985) p. 639
160. Stern O, Volmer M *Phys. Z.* **20** 183 (1919)
161. Kondrat'ev V N, Nikitin E E *Kinetika i Mekhanizmy Gazofaznykh Reaktsiĭ* (Kinetics and Mechanisms of Gas-Phase Reactions) (Moscow: Nauka, 1974)
162. Bibinov N K et al. *Khim. Fiz.* **5** 615 (1986)
163. Zuev V S et al. *Kvantovaya Elektron.* **8** 2183 (1981) [*Sov. J. Quantum Electron.* **11** 942 (1981)]